5

Investigating New Materials and Architectures for Grätzel Cells

Alex Polizzotti, Jacob Schual-Berke, Erika Falsgraf and Malkiat Johal*
Pomona College
USA

1. Introduction

A third-generation photovoltaic cell known as a Gratzel or Dye-Sensitized Solar Cell (DSSC) has been gaining attention due to its high lab efficiencies, ease of manufacture, and earth-abundant, nontoxic composition. These cells promise to be marketable in the near future, but several hurdles must still be overcome before Gratzel Cells can be mass-produced. This chapter outlines the technological theory behind Gratzel cells, summarizes the state-of-the-art of DSSC research, and identifies the major challenges that still must be addressed to reduce recombination and increase voltage, current density, and cell lifetime.

2. Grätzel cell overview

Some of the most promising photovoltaic technologies are the emerging third-generation technologies. These range from polymer cells to cells made from proteins extracted from jellyfish (Chiragwandi *et al*). One variety in particular, known as the Grätzel cell, has gained prominence due to its very low cost and ease of manufacture. Developed in 1992 by Michael Grätzel at the Ecole Polytechnique in Switzerland (O'Regan & Grätzel, 1991), these biomimetic devices represent a significant departure from typical silicon solar cells. Unlike p-n junction cells, Grätzel cells, also known as dye-sensitized solar cells (DSSCs), work much like a photosynthetic plant cell (O'Regan & Grätzel, 1991).

The heart of a DSSC is the dye, which operates much like chlorophyll in a photosynthetic plant cell. This dye, usually a ruthenium-based organometallic complex, is responsible for harvesting photons. When a photon hits the dye, an electron is excited from the ground-state (HOMO) into the first excited state (LUMO), leaving behind a hole. In other words, the dye is responsible for generating an exciton (O'Regan & Grätzel, 1991).

Just as with a silicon cell, the hole and excited electron will recombine if they are not separated. Thus, in order to ensure an efficient design the electron and hole must be quickly separated from each other to prevent recombination. This separation has two parts: first, the excited electron must be brought to one side of the cell – the anode. Second, the hole must be transported to the opposite side of the cell – the cathode.

The first part – transporting the electron – is typically performed by a titania (TiO_2) nanostructure and is known as the electron transport layer (ETL). This titania nanostructure is mesoporous, meaning that it has a pore structure on the order of 2-50 nanometers, and is annealed directly onto the anode. The dye molecules are introduced into this titania matrix

via immersion in a dye solution, where they chelate to the TiO_2 directly. When electrons are excited in the dye molecule, they are able to flow very quickly from the dye molecule LUMO into the lower-energy TiO_2 conduction band, where they flow down to the anode's conduction band, which is still lower in energy (Duffy *et al*., 2000). The importance of the nanoporous semiconductor layers, not only on electron transport, but also on increasing photon absorption are described in section 3.

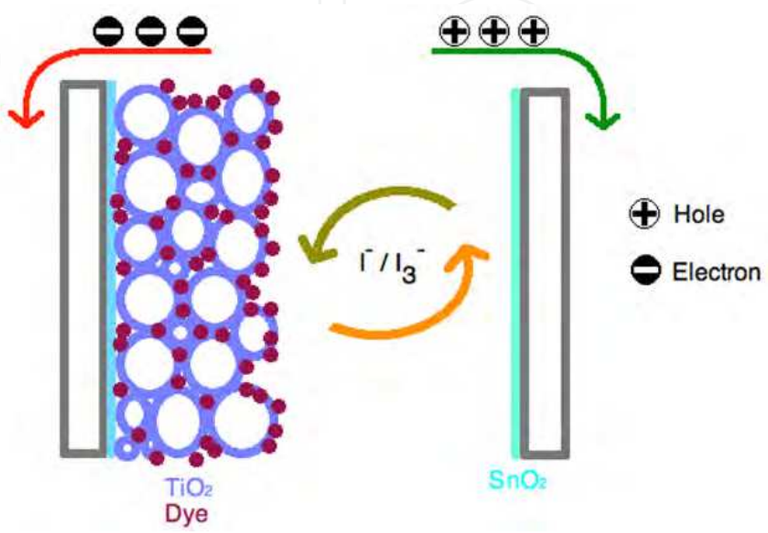

Fig. 1a. Structure of a Grätzel Cell. A mesoporous titania nanoscaffolding houses small dye molecules, which harvest light and generate excitons. Electrons flow through the titania to an anode mounted on glass substrate, and the dye's electrons are regenerated by the cathode via a redox couple such as I^-/I_3^-.

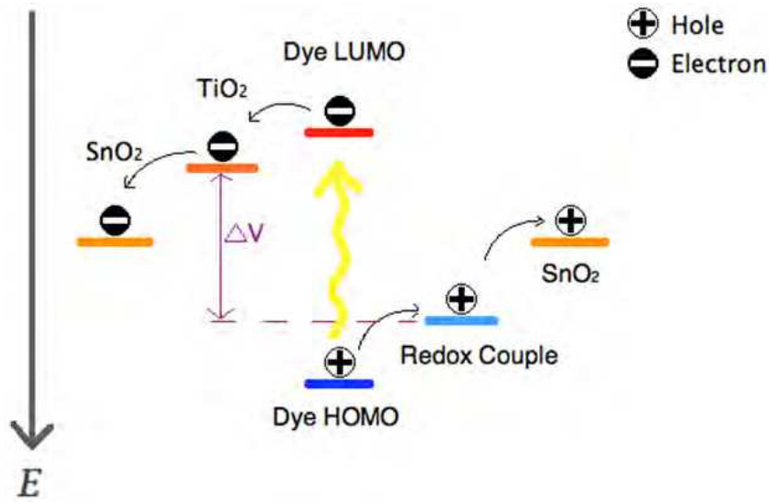

Fig. 1b. Typical energy diagram of a Grätzel Cell. Electrons are excited from dye HOMO to LUMO, where they transfer to the conduction band of the TiO_2 nanostructure, and on to the anode. Meanwhile, holes left in dye LUMO travel up in energy through the redox couple, and then up to the cathode. The maximum attainable voltage is believed to be approximately determined by the energy difference between the Fermi energy of illuminated electrons in the semiconductor and the redox energy of the HTL.

The second task – transporting the hole – is performed by the hole transport layer (HTL) and can be accomplished in a variety of ways. The first dye-sensitized cells created by Grätzel *et al*. utilized an iodide / triiodide redox couple, where iodide regenerates the oxidized dye molecules. The resulting oxidized species, mostly triiodide, are transported to the cathode via diffusion, where they are reduced back to iodide. In this way, positive charge carriers (holes) are transported from dye molecules to the cathode (O'Regan & Grätzel, 1991). A variety of new HTL materials have emerged since the first Grätzel cell, ranging from new liquid electrolytes through solid-state conjugated polymers to quasi-solid polymer-electrolyte mixes. The function of the HTL and ways to improve it are described in section 4.
Regardless of materials, the electrical characteristics of these cells are still not completely understood. The voltage, specifically, is not well explained in the literature (Li *et al*., 2011; Johansson *et al*., 2005). Voltage is, ultimately, the difference in work function under illumination of the two electrodes from which voltage measurements are taken. In other words, this voltage is a result of difference in electrochemical potential of mobile electrons under illumination at the electrodes (Cahen *et al*., 2000). In a DSSC, the electrochemical potential at the electrodes is primarily determined by differences in energy between the HTL and ETL - the maximum possible photovoltage is widely agreed to be the difference in energy between the Fermi energy of electrons in illuminated TiO_2 (roughly approximated as the conduction band edge) (Duffy *et al*., 2000), and the redox potential of the liquid electrolyte (O'Regan & Grätzel, 1991). In the case of a solid-state device, the difference between TiO_2 conduction band and the HOMO level of the HTL material determines the maximum voltage instead (Johansson *et al*., 2005).
However, the observed photovoltage is rarely this maximum value – for example, similar cells using Poly(3,4-ethylenedioxythiophene) poly(styrenesulfonate) (PEDOT:PSS) and poly(4-undecyl-2,20-bithiophene) (P3PUT) differ in photovoltage by 0.7 V, even though HOMO levels of these polymers lie 1 eV apart (Johansson *et al* 2005; Smestad *et al*., 2003). One of the major detractors of voltage is recombination, the process by which excited electrons and holes recombine, giving off energy as photons. This not only detracts from current, since it means fewer electrons doing useful work, but it also lowers the observed voltage (Ghadiri *et al*., 2010; Ito *et al*., 2008; Saito *et al*., 2004). Because recombination causes fewer electrons to reach the anode, the Fermi energy of electrons at the anode will be decreased. Similarly, fewer holes reaching the cathode will increase the energy of electrons at the cathode. Photovoltage, which is determined by the difference between the two electrodes, is therefore decreased. This and other factors can seriously affect the photovoltage, thus complicating the mechanism for establishing a photovoltage.
Though these cells are nascent and their properties still being explored and optimized, DSSCs have achieved moderate efficiencies of over 11%, which is encouraging given the extremely low cost of these cells. Although these cells are not yet marketable, improvements in each of the three main components (Dye, ETL and HTL), as well as improved reliability and lifetime, will help Grätzel cells to achieve their full industrial potential.

3. The sensitizer

The dye in a Dye Sensitized Solar Cell has one of the most fundamental tasks. This molecule is responsible for photon harvesting and generation of an exciton. The dye, in other words, uses light to create the charge separation that is the goal of any electrochemical cell. This dye, though a complex molecule, is very simple functionally: it must only satisfy a few key

requirements. The first of these is that it must absorb radiation across a broad visible spectrum. The second is that it must be small enough to enter the pores in the nanoporous semiconductor lattice. The third is that once inside the lattice, it must be able to chelate to the TiO_2 or other semiconductor. The last, and potentially the most challenging requirement, is that the dye must be able to accomplish the other three requirements while being cheap and environmentally benign.

The majority of incoming solar power is due to visible wavelengths. Thus, a dye must be able to absorb across these wavelengths – it must appear black. Porphyrin-based sensitizers have been shown to exhibit such effects. Figure 2 demonstrates the broad-spectrum absorption properties of N-719 and Z-907. Note that the wavelengths at which these dyes absorb photons are determined by the band gap properties of the dye, while the magnitude of the absorption is due to the molar absorption coefficient, ε, of the dye. In order for a dye to be effective, it must have a high value for ε in addition to exciting over a wide spectrum.

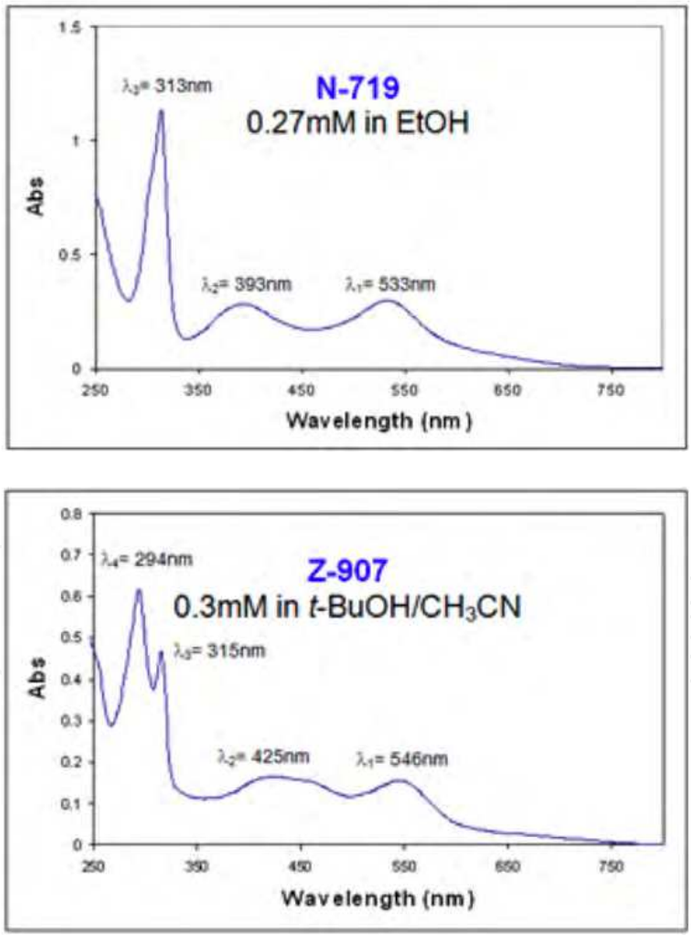

Fig. 2. UV/Vis absorption spectra of Ru-based dyes N719 and Z907. Reproduced from (Desilvestro & Hebting, 2011), with permission.

The second requirement of the dyes, that they must be able to enter the anatase structure, is relatively easy to satisfy. Though in the original Grätzel article the large size of the dye molecule prevented complete saturation of chelation sites (O'Regan & Grätzel, 1991), dye molecules are typically on the order of 1 nm in diameter (Katoh *et al*., 2010), and thus are easily able to penetrate into the 2-50 nm pores characteristic of mesoporous materials. Moreover, further work is being done into alternative semiconductor morphologies such as anatase nanotubes that will increase dye access to adsorption sites. This research is further discussed in section 3.

Third, the dye must be able to chelate to the semiconductor structure. This is usually accomplished via carboxylate or carboxylic acid groups, with the deprotonated species being far more soluble (N3 and N719 dyes, two of the most common, are identical except for this difference). Chelation can also be accomplished via phosphate and sulfonate groups (Johannsson *et al*., 2005).

3.1 Ruthenium dyes

Ruthenium-based dyes have met the described requirements (i.e., photon absorption, spreading in porous media and chelation to the semiconductor) superbly. Dyes made of ruthenium-based organo-metallic complexes have achieved overall conversion efficiencies of greater than 11% (O'Regan & Grätzel, 2004). The carboxyl moieties on the molecules allow them to chelate to the TiO_2 surface, they have broad-spectrum absorption, and exhibit high molar extinction coefficients. N3 (fig. 3), for instance, has absorption maxima at 518 and 380 nm with a high value of $\varepsilon = 1.35*10^4$ M^{-1} cm^{-1} in alkaline solution at 500nm (Katoh *et al*., 2010). N719, the partially deprotonated salt of N3, has near-identical properties ($\varepsilon=1.42*10^{-4}$ M^{-1} cm^{-1}) (G.W. Lee *et al*., 2010) plus enhanced solubility, while Z907 is a hydrophobic variant with two long photoactive carbon chains that shows broad absorption across the visible range. The structures of these dyes, along with that of N749, are shown in figure 3.

Further advancements in dye engineering have produced even more functional compounds. Many dyes are unable to absorb in the red wavelengths, but black dye (N749), with its three thiocyanate functional groups, absorbs wavelengths in the red and near IR range, giving it a dark brown-black color. Figure 4 shows that the photocurrent response of black dye extends to about 900 nm while that of N3 is attenuated in the range of 750-900 nm. Despite a lower value for ε of $7.7*10^3$ M^{-1} cm^{-1} (G.W. Lee *et al*., 2010), cells using black dye have achieved a conversion efficiency of 10.4% in full sunlight, approaching the maximum efficiencies of N3 (Grätzel, 2004), because of this spectral advantage. As well, Chiba et al. have built cells with black dye that yielded efficiencies of 11.1% when scattering particles were added to TiO_2 to increase haze (ratio of diffused transmittance to total optical transmittance) (Chiba *et al*, 2006). Other emerging ruthenium sensitizers include HY2, which has absorption peaks at 437 and 550nm with a molar absorption coefficient of 1.98 x 10^4 $M^{-1}cm^{-1}$ at the latter wavelength, significantly higher than that of N3 at its peak wavelength of 530nm. DSSCs with HY2 have attained efficiencies of 8.07% (Chen *et al*, 2009). A ruthenium sensitizer called K20 has recently been submitted for a patent with the remarkably high molar absorption coefficient of 2.2 x 10^4 $M^{-1}cm^{-1}$ at 520nm, a significant improvement over N3, N719, and black dye. Characterization of DSSCs sensitized with K20 has not yet been pursued (Ryan, 2009).

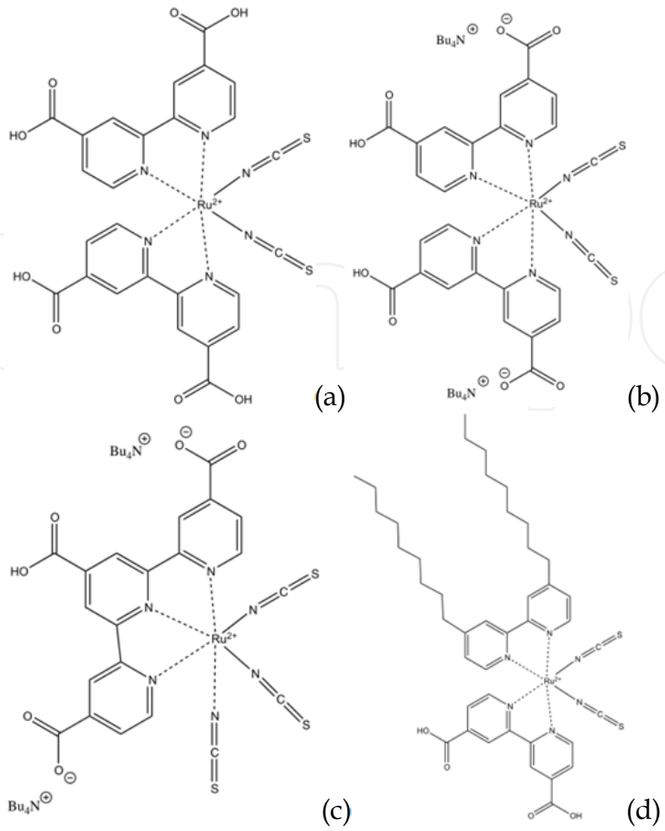

Fig. 3. Molecular structures of ruthenium complex dyes: (a) N3, IUPAC name cis-bis(isothiocyanato)bis(2,2'-bipyridyl-4,4'-dicarboxylato)-ruthenium(II); (b) N719, IUPAC name cis-diisothiocyanato-bis(2,2′-bipyridyl-4,4′-dicarboxylato) ruthenium(II) bis(tetrabutylammonium); (c) Black dye (N749), IUPAC name triisothiocyanato-(2,2′:6′,6″-terpyridyl-4,4′,4″-tricarboxylato) ruthenium(II) tris(tetra-butylammonium); and (d) Z907, IUPAC name cis-disothiocyanato-(2,2′-bipyridyl-4,4′-dicarboxylic acid)-(2,2′-bipyridyl-4,4′-dinonyl) ruthenium(II).

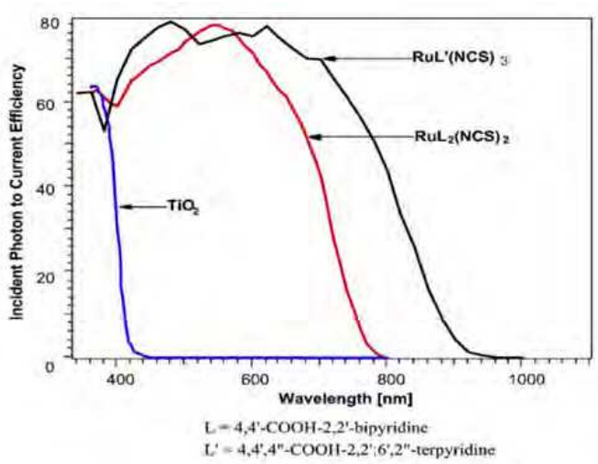

Fig. 4. Photocurrent action spectra of N3 (ligand L), black dye (ligand L′), and bare TiO_2. Reproduced from (Grätzel, 2004), with permission.

All of these dyes have several beneficial shared properties. Ruthenium-based complexes exhibit metal-to-ligand charge transfer, a process in which the excited electron in a d-orbital of Ru is transferred to the π^* orbital of the carboxyl ligand, from which it is injected into the conduction band of TiO_2. This transfer is fast and irreversible, and will be discussed further in section 3. Moreover, they are remarkably stable over long periods of time. In the 1991 article by Grätzel and O'Regan, dyes sustained $5*10^6$ turnovers without serious decomposition (O'Regan & Grätzel, 1991). More modern dyes are even more stable - in its solid state, N3 can withstand temperatures up to 280°C, and maintains high performance over 10^8 redox cycles, the equivalent of 20 years of use in sunlight (Grätzel, 2004).

If pure functionality were the only requirement for these dyes, then perhaps alternatives to these existing dyes would not be needed. However, the last and most difficult requirement is that these dyes must be cheap, nontoxic, and environmentally benign. The greatest barrier to such a dye is the use of ruthenium as a metal center in these metal complex dye molecules. World production of ruthenium is approximately 12 metric tons (Lenntech), and though it is found in the rare minerals laurite, ruarsite, and ruthenarsenite, its commercial recovery is limited almost entirely to trace elemental amounts in nickel deposits in Africa and the Americas. Due to its rarity in difficulty to obtain, Ruthenium is expensive even in small quantities. For instance, a 10 mg sample of N-3 from Solaronix currently costs approximately $244 USD (Solaronix.com as Ruthenizer 535). Moreover, ruthenium complexes are potentially hazardous to health and the environment. Though not yet fully studied for toxicity in their own right, when heated in air ruthenium complexes form ruthenium tetroxide, a highly volatile and toxic compound that damages the eyes and the upper respiratory system (Dierks, 2006). For all these reasons, a variety of entirely organic dyes as well as dyes using different metal centers are being developed for use in DSSCs.

3.2 Ru-free porphyrin dyes

Several main approaches have emerged to bypass the need for ruthenium dyes. One of the most common is to modify the dye structure to allow for a different metal center such as zinc or magnesium. Porphyrins, a class of naturally occurring biological compounds that include chlorophyll and hemoglobin, are known to absorb radiation in the visible range due to a conjugated system of pyrolles, frequently complexed around a metal ion center (iron in the case of hemoglobin, and magnesium in the case of chlorophyll). As chlorophyll is the biological inspiration for many of the dyes in DSSCs today, much work is being done currently to produce porphyrin-based, ruthenium-free organometallic dyes. The Grätzel lab recently developed a porphyrin dye called YD-2 that achieved an 11% power conversion efficiency in a 16μm TiO_2 layer, the highest efficiency demonstrated by a ruthenium-free sensitizer. The structure of YD-2 is shown in figure 5.

Moreover, chlorophyll itself is relatively simple to modify, which allows researchers to create highly biomimetic devices while manipulating properties such as excited-state lifetime and LUMO energy level as well as enhance adsorption to TiO_2 (Wang *et al.*, 2010b). Chlorophyll (Chl) comes in several distinct forms, most commonly Chl *a*, Chl *b*, and Chl *c*; the latter two are typically found as accessory pigments in light-harvesting complexes, which serve to absorb additional solar radiation and transport excited electrons to the reaction center, which contains Chl *a*. (Figure 6a). In an effort to mimic the multimolecular approach used by plants to harvest light, researchers constructed DSSCs with co-sensitized Chl derivatives, which were labeled *a*-type, *b*-type, or *c*-type depending on which Chl they structurally resembled. Combinations of *a*-type Chl sensitizers with *c*-type Chl sensitizers

resulted in augmented power conversion efficiencies of 5.4% (Wang *et al*., 2010a). This group subsequently developed a Chl-*a* derivative, chlorin-3, with a dodecyl ester group at C17, where a carboxyl group would normally be. DSSCs with chlorin-3 obtained a conversion efficiency of 8% with an AcCN redox electrolyte HTL, the highest efficiency for any chlorophyllous sensitizer to date. (Wang *et al*., 2010b).

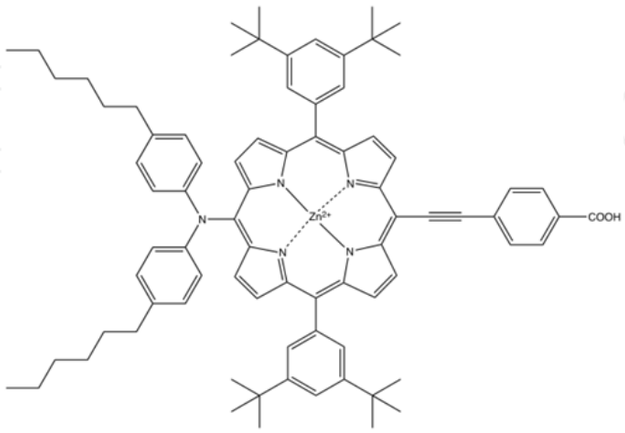

Fig. 5. Molecular structure of YD-2.

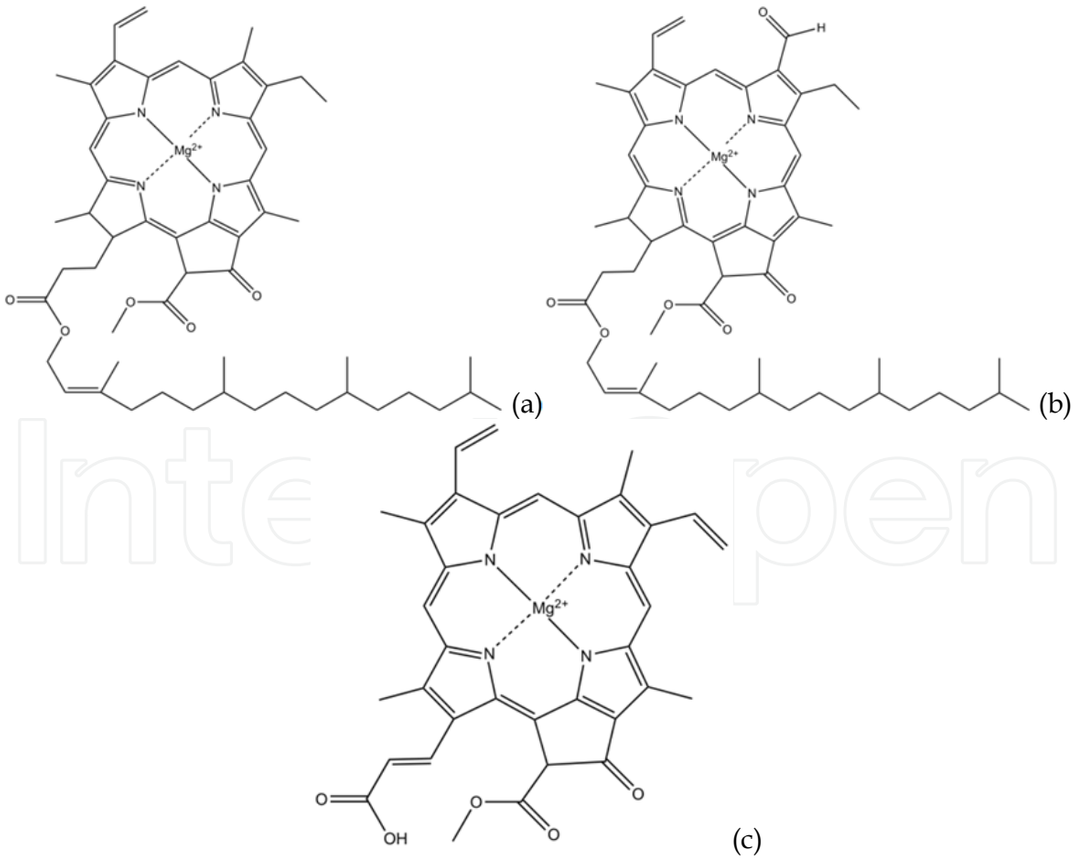

Fig. 6. Molecular structures of some chlorophyll: (a) Chlorophyll *a*; (b) Chlorophyll *b*; and Chlorophyll *c2*.

3.3 Fully organic dyes

Another fast-growing method for doing away with ruthenium in sensitizers is to create completely organic sensitizers without the need for a metal center at all. Indoline sensitizers such as D149 show promise for their extremely high molar absorption coefficient of 6.87 x 10^4 $M^{-1}cm^{-1}$ at 526 nm. DSSCs with D149 have achieved efficiencies of 9.0% and 6.7% in cells with acetonitrile-based electrolytes and cells with ionic liquid (IL) electrolytes, respectively (Ito *et al*., 2006). Subsequent work using the indoline sensitizer D205 with IL electrolytes achieved an efficiency of 7.2%, the highest efficiency obtained in DSSCs with organic dyes and an IL HTL (Kuang *et al*., 2008).

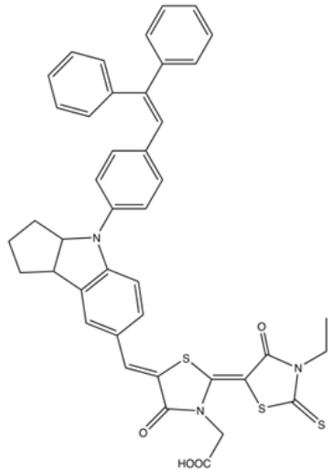

(a)

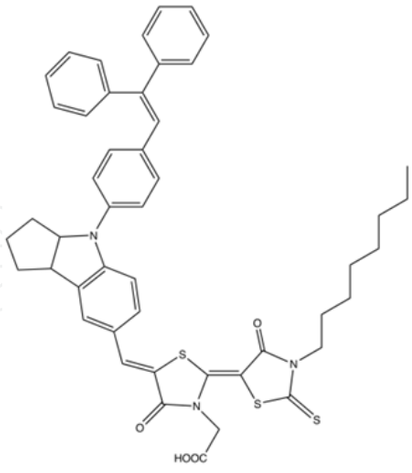

(b)

Fig. 7. Molecular structures of indoline sensitizers: (a) D149; and (b) D205.

Yum *et al* have demonstrated efficiencies of 7.43% and respectable absorbances in the red/near IR region using cells cosensitized with JK2 and SQ1, both organic, non-porphyrin molecules (Figure 8). JK2 and SQ1 have impressive molar absorption coefficients of 4.2 x 10^4 $M^{-1}cm^{-1}$ at 452 nm and 15.9 x 10^4 $M^{-1}cm^{-1}$ at 636 nm, respectively (Yum et al., 2007).

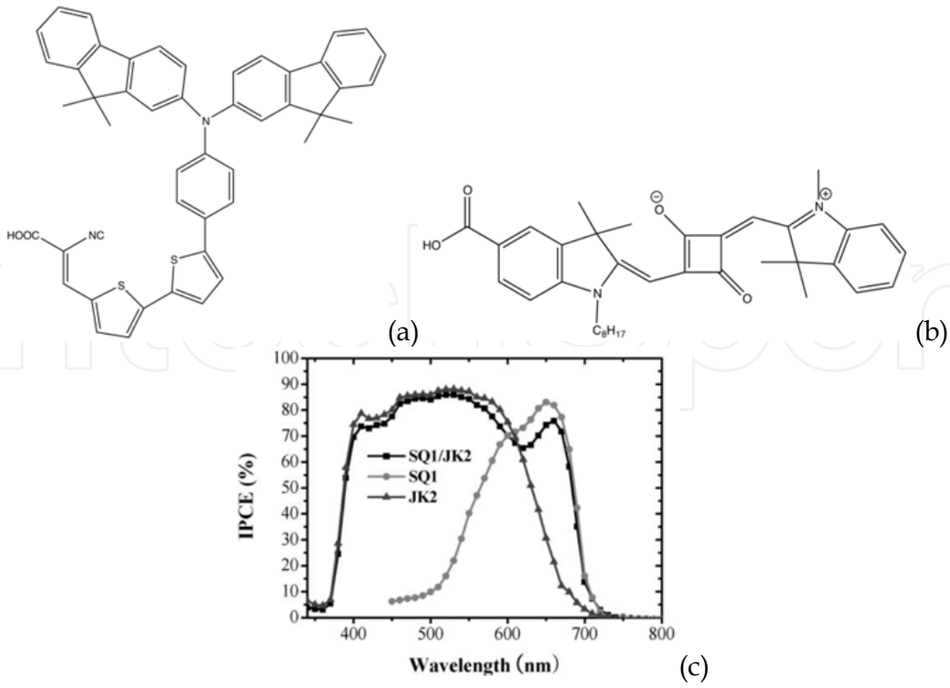

Fig. 8. (a) Structure of JK2; (b) structure of SQ1; and (c) IPCE profile of cells sensitized with SQ1 (light gray), JK2 (dark gray), and SQ1/JK2 (black). Graph reproduced from (Yum *et al*., 2007), with permission.

Advanced dye engineering has produced superior organic dyes. However, the simplest of these molecules can be found as the colorful dyes in berries and flowers. Anthocyanins and betalains are two classes of biological molecules being investigated for their photoactive properties. Anthocyanins are colorful flavonoids that are found in fruits such as blackberries and raspberries. Though they can be modified - their energy absorption is pH sensitive with acidic solutions turning many anthocyanins into a red dye (Calogero *et al*., 2009) – their overall conversion efficiencies are quite low. DSSCs sensitized with juice from red Sicilian oranges (*Citrus Sinensis*) achieved an efficiency of 0.66%(Calogero & Di Marco, 2008). Nevertheless, anthocyanins are easily extracted from plants and are both abundant and diverse. Betalains are found in Caryophyllales plants, which include red turnip, wild purple sicilian prickly pear, and bougainvillea flowers. Betalain pigments include betanine, which has a red-purple coloration, and betaxanthins, which are yellow-orange; both compounds have carboxyl functional groups, allowing them to readily chelate to TiO_2. DSSCs sensitized with betalains from red turnip yielded an overall conversion efficiency of 1.75%, a remarkable value for nonsynthetic, biological dyes (Calogero *et al*., 2009). These biological sensitizers are in the initial stages of development and may be a nontoxic and inexpensive option for DSSCs of the future.

Long-term stability is a factor to consider for all dyes, and the stability of ruthenium complexes is the main reason that they are still the standard sensitizers in high-performance DSSCs. However organic dyes are also gaining the potential to exhibit long-term stability; a sensitizer called D21L6 sustained 1000 hours of light soaking at 60°C and maintained an efficiency of 90% of the initial value, an unprecedented degree of stability for organic sensitizers. Furthermore, D21L6 has a molar absorption coefficient of 3.7×10^4 $M^{-1}cm^{-1}$ at 458

nm, superior to ruthenium-based dyes, and have achieved overall conversion efficiencies of 7.25% and 4.44% in cells with AcCN electrolytes and solid-state HTL material, respectively (Yum et al., 2009). This combination of stability and efficiency indicates that D21L6 and other organic dyes may be able to replace ruthenium complexes as the preferred dyes in DSSCs.

The high price and limited availability of ruthenium dyes is one of the main drawbacks to DSSCs. However, new advancements in dye fabrication promise to take the ruthenium out of Grätzel cells and significantly improve their watt-to-cost ratio. Though ruthenium dyes are still the most commonly used dyes, both organic and porphyrin-based organometallic dyes are poised to become the cheap and nontoxic alternatives for future cells.

4. The Electron Transport Layer (ETL)

Sensitizers generate excitons, thus creating the initial charge separation that is vital to the function of any solar cell. However, these excitons are very short lived, and excited electrons tend to recombine with the holes to which they are still coulombically (i.e. electrostatically) bound. Thus, an effective semiconductor electron-transport matrix is essential in a DSSC to efficiently separate charge.

Optically transparent microfilms of anatase TiO_2 (and some other metal oxide semiconductors such as ZnO) have been found to effectively transport charge from an excited dye to an electrode. However, charge transport alone is insufficient. A monolayer film of dye adsorbed onto a one-dimensional TiO_2 layer yields very low-efficiency solar cells, well below 1% (O'Regan & Grätzel, 1991). This low efficiency is due to the poor absorption properties of dyes in a monolayer – less than 1% of incident light is absorbed by a monolayer of dye on a flat TiO_2 surface (O'Regan & Grätzel, 1991).

Though Grätzel cells differed from previous dye-sensitized photoelectrical cells by introducing a more efficient dye, the true innovation that made the first Grätzel cell so significant was the use of a highly mesoporous (pores in the range of 2-50 nm) semiconductor layer. This layer, fabricated by the deposition of TiO_2 or another metal oxide semiconductor in a colloidal solution followed by drying and sintering, allows dye to be adsorbed in the pores of the semiconductor, thus vastly increasing the amount of dye adsorbed onto the material. Figure 9 shows scans of a typical anatase mesoporous film.

To give an idea of the impact of such a mesoporous layer, the 10 micrometer thick layer of 15 nm average diameter TiO_2 particles used in the original Grätzel cells, packed cubically, is expected to have a roughness factor of 2000. In other words, these films are expected to produce a 2000-fold increase in surface area as opposed to a perfectly flat film. In reality, Grätzel and O'Regan found that this first attempt at a mesoporous TiO_2 anode only produced a roughness factor of 780 (O'Regan & Grätzel, 1991). This discrepancy was attributed to "necking" – inter-particle fusions that decrease surface area – as well as the fact that some parts of the porous structure were too small for the relatively large dye molecules to penetrate. Regardless of these imperfections, a new method had been demonstrated for extremely high adsorption of dye molecules into a small area while still allowing contact between dye and liquid electrolyte. With this remarkably simple mechanism, which allowed for 7% efficiencies in ambient sunlight, and 46% harvesting of incident photons (O'Regan & Grätzel, 1991), dye-sensitized photoelectrical cells began to show real promise of future commercial viability.

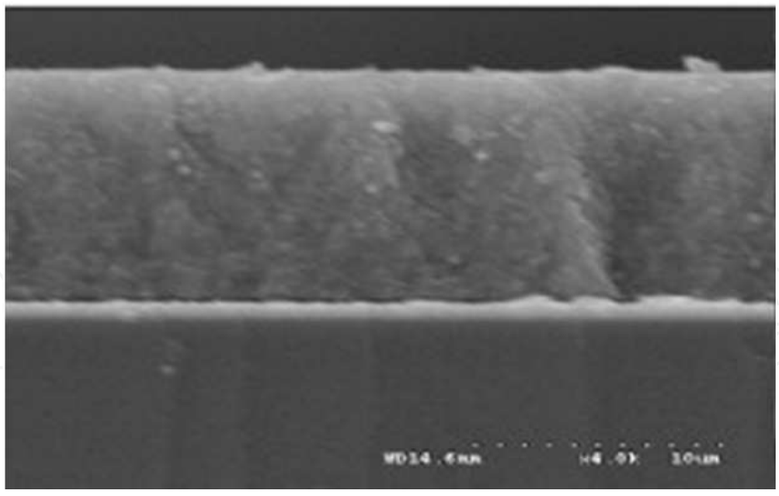

a)

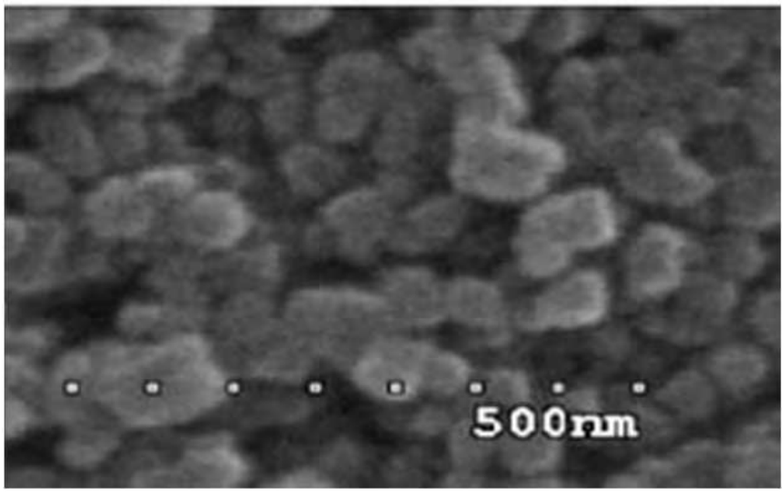

b)

Fig. 9. a) cross section view and b) top view of SEM scans of anatase TiO_2 films prepared via doctor blade method. Reproduced from (Singh *et al*., 2008), with permission.

One great advantage to a mesoporous TiO_2 structure aside from higher dye packing is its ability to trap light within its pore structure. Instead of photons hitting a flat surface (and either being absorbed or reflecting away), unused photons are scattered by TiO_2 nanoparticles until they either escape or are absorbed by a dye molecule. This process repeats, immensely increasing a photon's chance of interacting with dye. As opposed to the 1% light harvesting efficiency seen on a flat ETL, recent papers have achieved over 95% harvesting of incoming photons (Ghadiri *et al*., 2010).

Mesoporous TiO_2 layers are effective because they allow for very dense dye adsorption, and increase the path length of light inside their porous structure. These factors contribute to a sufficiently high rate of exciton generation upon illumination – in other words, photons have a high probability of reflecting around inside the crystal TiO_2 structure until

they hit one of the densely adsorbed dye molecules. However once this occurs, the TiO_2 must then accept this excited electron from the dye and also transport the excited electron to the anode before it has a chance to recombine with holes in the oxidized dye or in the HTL.

The driving force behind electron injection into the TiO_2 from the dye is twofold. Firstly, there is an enthalpic impetus to electron injection from dye LUMO to the TiO_2 conduction band. Because the conduction band lies below the dye LUMO in energy, it is energetically favorable for an electron to transport from dye to TiO_2 immediately upon excitation (Cahen *et al*., 2000; Liu *et al*., 2002). The energy gap $E_{LUMO} - E_{CB}$ between the two materials determines the strength of the enthalpic driving force. For a typical dye such as N3, which has a LUMO energy of -3.74 eV vs. vacuum (Nazeeruddin *et al*., 1993; Zafer *et al*., 2005), injecting electrons into mesoporous anatase TiO_2 with conduction band edge at -4.1 eV vs vacuum (Cahen *et al*., 2000; Liu *et al*., 2002; Tang *et al*., 1994), this energy difference is ~0.34 eV.

The second impetus to electron injection from dye to TiO_2 is entropic. Per unit area, anatase TiO_2 has a much higher density of possible electronic states than the dye molecule. Thus, an electron diffusing from dye to TiO_2 causes a gain in entropy, much like a gas molecule flowing from a small container to a large container. This entropy gain can result in an additional, substantial driving force of up to ~0.1 eV (Cahen *et al*., 2000).

The advantage of these two driving forces – entropic and enthalpic favorability – is that they are essentially irreversible. Reverse transport of electrons from the TiO_2 conduction band edge to dye LUMO is unlikely (O'Regan & Grätzel, 1991; Cahen *et al*., 2000). Moreover, since there are essentially no minority charge carriers in TiO_2 (i.e. there are no free holes in the TiO_2), recombination within the semiconductor is unlikely (O'Regan & Grätzel, 1991). The implication is that rough or broken TiO_2 films can still produce perfectly functional Grätzel cells. Limiting recombination is key for a solar cell – as discussed in the introduction, though open-circuit voltage (V_{oc}) is primarily determined by the energy difference between ETL Fermi energy upon illumination and HTL oxidation potential (Nernst potential in the case of a liquid electrolyte redox couple), recombination detracts from this value significantly (Ghadiri *et al*., 2010; Li *et al*., 2011; Peng *et al*., 2004;).

Thus, the majority of recombination in a Grätzel cell is due to interactions between electrons in the TiO_2 semiconductor and anode material, and holes in the HTL. For a liquid iodine redox couple, this means that oxidized species of iodine, such as I_2^- and I_3^-, can absorb electrons in the TiO_2 matrix. However, this recombination requires electrons in the TiO_2 nanostructure to be within tunneling distance of the HTL (Cahen *et al*., 2000), or within approximately 3 nm. In a system where particles have an average diameter of 20 nm, this means that only electrons on the surface of TiO_2 particles have the possibility of recombining at all. Moreover, this implies that the recombination rate is inversely proportional to particle size, and directly proportional to the specific surface area.

There are other mechanisms that prevent recombination in Grätzel cells. Among the most important of these is ionic screening in a liquid electrolyte cell. Iodine and counterions shield holes in the HTL and electrons in the ETL from their coulombic attraction, thus decreasing the likelihood that these particles will recombine (Cahen *et al*., 2000).

These and other lesser mechanisms make for a very low rate of recombination in Grätzel cells, especially those employing a liquid electrolyte (O'Regan & Grätzel, 1991; Cahen *et al*., 2000; Peng 2004). This low recombination rate results in a relatively high fill factor (i.e. the

ratio of observed efficiency to theoretical max efficiency). The fill factor for the first DSSC was 0.684 (O'Regan & Grätzel, 1991), and recent cells attain values of up to 0.75 (Ghadiri *et al*., 2010). To give a comparison, the fill factor for an average commercial silicon cell is ~0.83, while some advanced inorganic thin-film cells have achieved almost 0.90 (Green, 1981; PVEducation.org). Grätzel cells therefore compare very favorably with current commercial cells in this respect.

Thus, four important characteristics have emerged that work to make a TiO_2 mesoporous semiconductor layer more effective than a flat electrode. First, the TiO_2 nanostructure provides a very high effective surface area for dye molecule adsorption due to its very high roughness factor. Second, the TiO_2 provides very favorable and effectively irreversible entropic and enthalpic driving forces for charge injection. Third, low recombination within the semiconductor matrix as well as between the semiconductor and the HTL allows for very efficient electron transport to the anode. Fourth, light scattering within the porous crystalline structure increases the radiation path-length and thus improves photon harvesting. And, because of the porous nature of the ETL, this all happens while simultaneously allowing the HTL to come into direct contact with every single dye molecule just like for a flat electrode (O'Regan & Grätzel, 1991).

4.1 Improving the ETL through new morphologies

These four main requirements have guided efforts to improve ETL function further. If dense adsorption of dye onto TiO_2 is responsible for the efficiency of the original Grätzel cells, then increased-surface-area materials and more favorable dye-semiconductor adsorption interactions can make these cells even more effective. Likewise, finding ways to prevent recombination, increase light scattering, and increase the driving force for charge injection will further increase cell performance.

The use of light-scattering semiconductor particles is one of the simplest and easiest ways to improve device efficiency. Ito *et al.* used larger TiO_2 particles on top of a mesoporous TiO_2 layer to scatter photons into the semiconductor pores, increasing path-length of the photons and increasing cell efficiency substantially (Ito *et al*., 2007).

Other methods have emerged to prevent recombination rates in Grätzel cells. One major problem is contact between the hole-rich HTL and the electron-rich photoanode. In solid-state devices, which use a solid HTL, this is an even larger problem. In the original Grätzel cells, liquid electrolyte provided ionic screening to prevent charge recombination. In a solid device, this phenomenon does not occur. Moreover, some solid HTLs cause a short circuit by providing direct electrical contact between anode and cathode, thus rendering the device non-functional (Peng *et al*., 2004). A simple solution to this problem is the use of a nonporous semiconductor layer in between the anode and the mesoporous semiconductor layer, shown in figure 10. While providing electron transport in the same fashion as the mesoporous layer, this nonporous "blocking" layer prevents HTL material, whether liquid electrolyte or solid material, from directly contacting the anode (Peng *et al*., 2004; Saito *et al*, 2004). Work by Peng *et al*. has shown that a blocking layer of TiO_2 can significantly prevent charge recombination at the anode, and that the ideal thickness for a blocking TiO_2 layer is between 120 and 200 nm (Peng *et al*., 2004). Since the porous layer of titania is on the microscale – typically 10 or more micrometers, this study shows that a significant increase of efficiency is possible using only minimal extra amounts of material.

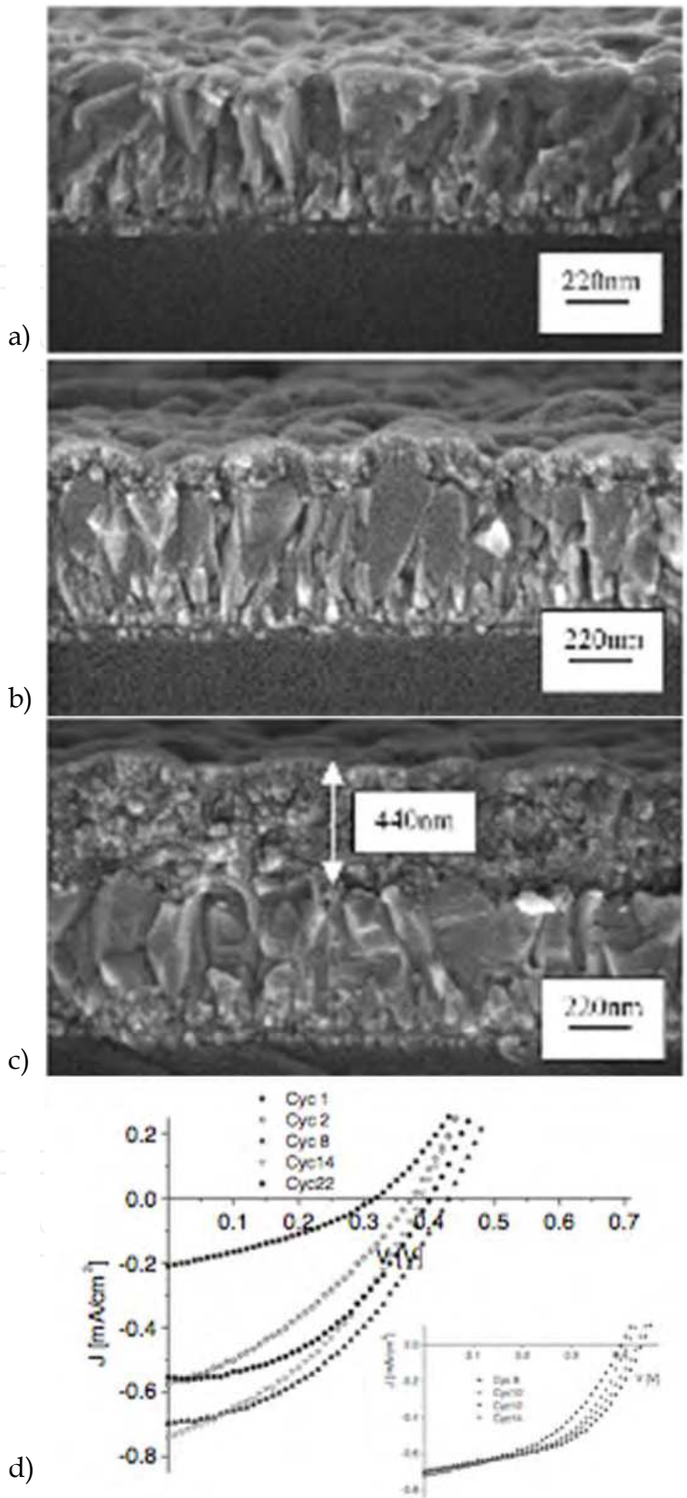

Fig. 10. a) Bare FTO electrode compared to b) 8 and c) 30 spraying cycles of blocking TiO_2. d) I-V curves of cells made with blocking TiO_2 films. Performance is optimized between 8 and 14 spraying cycles. Reproduced from (Peng *et al*., 2004), with permission.

4.2 Semiconductor nanotubes as ETL

One ETL technology that has been gathering interest recently is the use of semiconductor nanotubes. One of the problems with mesoporous films is that cracks and gaps between TiO_2 particles in the anatase layer create electron traps (Ghadiri *et al*., 2010; Li *et al*., 2011). In other words, gaps between nanoparticles in the mesoporous structure make it difficult for electrons to tunnel from particle to particle, thus retarding electron movement through the semiconductor (Mor *et al*., 2006). This slowing of electrons gives rise to a higher probability of recombination with holes in the HTL. One-dimensional electron transport via semiconductor nanotubes seeks to remedy this problem. Adachi *et al.* reported efficiencies of 4.88% using disordered nanotube arrays in 2003 (Adachi *et al*., 2003). Mor *et al*. reported the use of highly-ordered TiO_2 nanotubes for improved electron transport in 2006. Though their devices exhibited only 2.9% efficiencies, this was for a nanotube layer only 360 nm thick, or under 1/30 the thickness of the original 10 micrometer films used by Grätzel and O'Regan (Mor *et al*., 2006; O'Regan & Grätzel, 1991). They noted that efficiency scaled linearly with nanotube length, meaning that dye adsorption appears to be the limiting factor. They hypothesized that with several-micrometer-long nanotubes this system has an ideal limit of ~31% efficiency (Mor *et al*., 2006). SEM scans of nanotube systems are shown in figure 11.

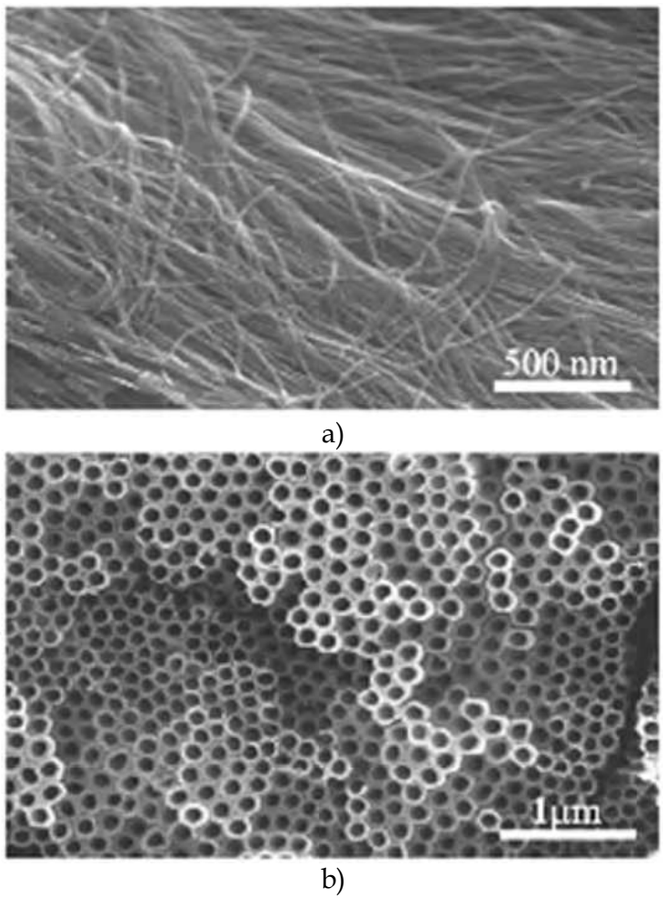

Fig. 11. SEM scans of TiO_2 nanotubes a) without treatment and covered with a layer of nanowires and b) after ultrasonic treatment in ethanol to remove nanowires. Reproduced from (Li *et al*., 2011), with permission.

The reason for this high ideal efficiency with nanotubes is due to their simple linear architecture. A nanotube, unlike a mesoporous TiO_2 layer, provides very direct and one-dimensional electron transport (Bendall *et al*., 2011; Ghadiri *et al*., 2010; Li *et al*., 2011). The small boundary between TiO_2 particles **in** highly-ordered nanotubes largely bypasses the problem of electron traps caused by gaps in mesoporous structures. Because of this, the average length an electron can travel in these tubes before recombining, known as the diffusion length, is much longer (Ghadiri *et al*., 2010; Li *et al*., 2011). It has been estimated by Jennings *et al.* that the diffusion length in a nanotube cell is approximately 100 micrometers (Jennings *et al*., 2008). As many nanotube layers in this kind of study have only reached 20 micrometers or less, there is great potential for scaling up tube size, and thus effective surface area, without significantly increasing the rate of recombination.

Additionally, nanotubes are more "open" than mesoporous layers. This means that oxidized species in the liquid electrolyte can quickly escape from the tube structure as opposed to being trapped in the pore structure. Once the electrolyte accepts a hole from the dye, it can quickly move to the cathode and be reduced, and thus has less chance of recombining with electrons in the ETL (Ghadiri *et al*., 2010, Li *et al*., 2011).

One of the downsides to carbon nanotubes is their high manufacturing cost. They usually require much more energy input than mesoporous layers, and are more time-consuming to fabricate (Bendall *et al*., 2011; Li *et al*., 2011). Thus, efforts are being made to decrease cost of these cells while increasing efficiency.

Hollow TiO_2 fibers were recently fabricated by Ghadiri *et al.* through a nanotemplating method, shown in figure 12. By creating cellulose nanofibers, coating them in TiO_2, and then removing the fibers via heat treatment, this group produced hollow TiO_2 fibers similar to nanotubes via a very cheap and effective method (Ghadiri *et al*., 2010), outlined in figure 13. Moreover, these structures were shown to have 2-3 times faster electron transport than mesoporous films, higher voltage due to lower recombination (despite nanofiber energy actually being *closer* to electrolyte Nernst potential than mesoporous films), and high efficiencies. In fact, cells made with fibers only 20 micrometers long exhibited 7.2% efficiencies, nearly identical to similar devices made with TiO_2 nanoparticles (Ghadiri *et al*., 2010). There are downsides to this technology, including lower roughness factors and less light trapping than mesoporous TiO_2. These problems can be mitigated by more efficient dyes (thus reducing the need for high-density adsorption), and decreasing fiber diameter to increase surface area. Nevertheless, despite these drawbacks nanotube cells performed similarly to mesoporous ETL cells. Thus, this technology has great potential for improvement and has promise to play a role in future generations of DSSCs.

Nanowires are a variation on the theme of highly-ordered nanostructures for the ETL. ZnO nanowire and nanotube fabrication require much milder conditions than for TiO_2 nanowires and nanotubes, and thus are an attractive option for their low cost of manufacture (Bendall *et al*., 2011). ZnO also has improved electron mobility as compared to TiO_2, which would lead to potentially longer diffusion length. Generally, ZnO exhibits lower affinity for dye adsorption, and tubes made from ZnO are less stable. However, Bendall *et al.* reported 2.53% efficiency using a mix of ZnO and TiO_2 nanowires, and reported effective dye adsorption with use of a novel organic dye (Bendall *et al*., 2011). Thus, ZnO remains a potentially attractive alternative to TiO_2 as the ETL material.

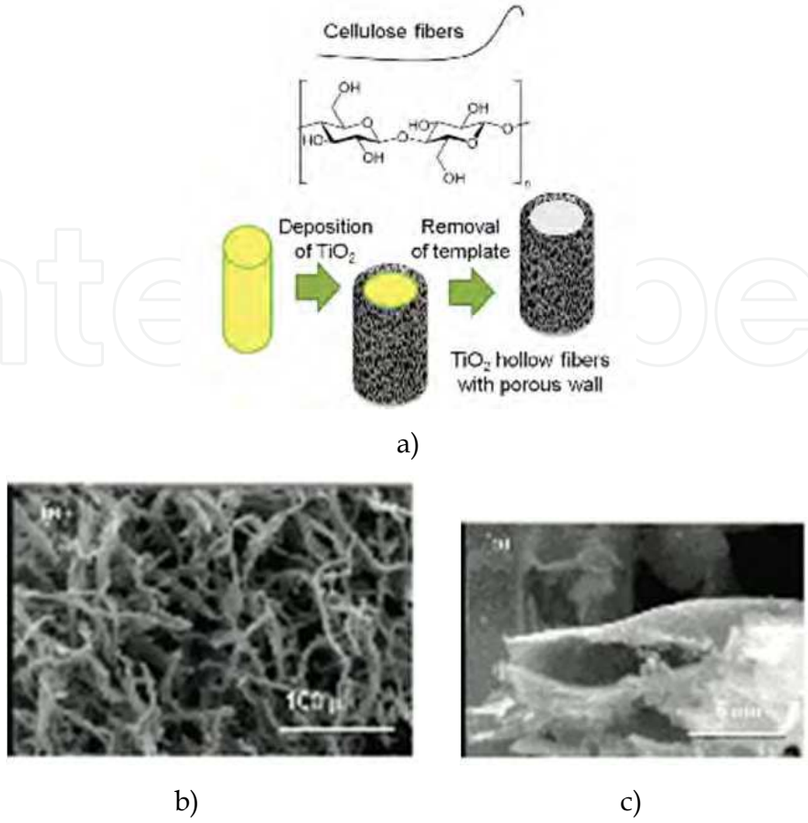

a)

b) c)

Fig. 12. a) Creation of porous hollow anatase fibers using a template method. b) SEM scan of hollow fibers immediately after template removal. c) cross section SEM scan of one hollow fiber. Reproduced from (Ghadiri *et al.*, 2010), with permission.

The ETL of a Grätzel cell, though usually made of just one material, is as vital as it is simple. Superior surface area allows for hundreds of times more dye to adsorb to surfaces than a flat ETL. Light trapping increases the likelihood that photons will interact with dyes. Low recombination rates due to unfavorable back-reactions combined with protective surface morphologies result in very high fill factors. And while performing all these tasks, anatase and ZnO semiconductor matrices allow light and HTL materials to contact the dye fairly unhindered. New developments in nanotubes and nanowires take these properties to the next level. They allow ultrafast, one-dimensional electron transport from dye to anode while still providing very efficient dye packing and easy access to HTL materials. New breakthroughs in low-cost nanotubes, higher-efficiency mesoporous layers, and nanowires, along with alternative ETL materials such as ZnO, continue to raise the efficiency of Grätzel cells, lower their cost, and further elucidate their inner workings.

5. The Hole Transport Layer (HTL)

The HTL in a DSSC plays a critical role in determining the device's efficiency, closed-circuit voltage, photocurrent and physical architecture. An effective HTL must be able to transfer charge rapidly so as to be able to regenerate the dye quickly and mitigate losses due to charge recombination between oxidized dyes and injected electrons (Hao *et al.*, 2011). In

addition, the material must be stable over long periods of time and elevated temperatures in the cell's operating range, around 80-85 °C (Wang *et al*., 2003). Though the most common and efficient HTL materials to this date are liquid electrolytes, a wealth of new and innovative research is being done on a wide variety of materials to make hole transport cheaper, more effective, and more robust (Helgesen *et al*., 2009).

5.1 Electrolyte redox couples as HTL

In the original DSSC design described in Grätzel's seminal 1991 publication, the cell utilized an I^-/I_3^- redox couple composed of tetrapropylammonium iodide, iodine, ethylene carbonate and acetonitrile. While the iodine is the active component of the redox shuttle, the other components are necessary to create a liquid electrolyte. Using this formulation, even without any of the significant improvements that have been developed in recent years, the cell exhibited an impressive efficiency in the range of 7-8% (O'Regan & Grätzel, 1991). This relatively high efficiency is due to the excellent mobility of the liquid electrolyte and its ability to make contact with, and rapidly regenerate, the dye inside the ETL. In a follow-up paper, Grätzel also demonstrated the significance of the electrolyte composition by showing that the I^-/I_3^- counterion (e.g. Li^+, tetrapropylammonium) had a significant effect on the photocurrent of the system (Kay & Grätzel, 1996) due to the improved ionic screening provided by these counterions. Among the iodide salts that form room-temperature ionic liquids, 1-propyl-3-methylimidazolium iodide (PMII) has the lowest viscosity, making it the most effective and widely used liquid electrolyte HTL (*vide infra*) (Bai *et al*., 2008).
The role of iodide in the electrolyte is to regenerate oxidized dye according to the following reduction reactions:

$$Dye^+ + 2I^- \rightarrow I^-_2 + Dye \quad (1)$$

$$2I^-_2 \rightarrow I^-_3 + I^- \quad (2)$$

The resulting triiodide must diffuse away to the cathode where it is reduced back to iodide according to the equation

$$I_3^- + 2e^- \rightarrow 3I^- \quad (3)$$

Thus, the diffusion coefficients of iodine and triiodide are very important in determining the rate at which the electrolyte can regenerate the dye and prevent recombination (Hao *et al*., 2011). The diffusion coefficients are a function of physical diffusion and exchange reaction constants. Physical diffusion is dictated by viscosity, which increases with electrolyte concentration due to ionic and van Der Waals interactions. A more viscous solution inhibits I^-/I_3^- diffusion, which reduces its ability to regenerate the dye. However, a high electrolyte concentration is necessary to yield sufficient ionic conductivity and enhances the rate of exchange reactions, so there is some optimal electrolyte concentration that balances these factors. Using a binary electrolyte system consisting of 1-ethyl-3-methylimidazolium dicyanamide (EMIDCA) / PMII with a fixed iodine concentration and a varying EMIDCA volume fraction, Lin *et. al*. concluded that a volume fraction of 40 vol% EMIDCA produced the maximal balance between physical diffusion and exchange reactions, leading to the optimal electrolyte composition. Indeed, when fabricated into a working cell, this electrolyte led to the highest efficiency of 5.20% (Figure 13) (Hao *et al*., 2011).

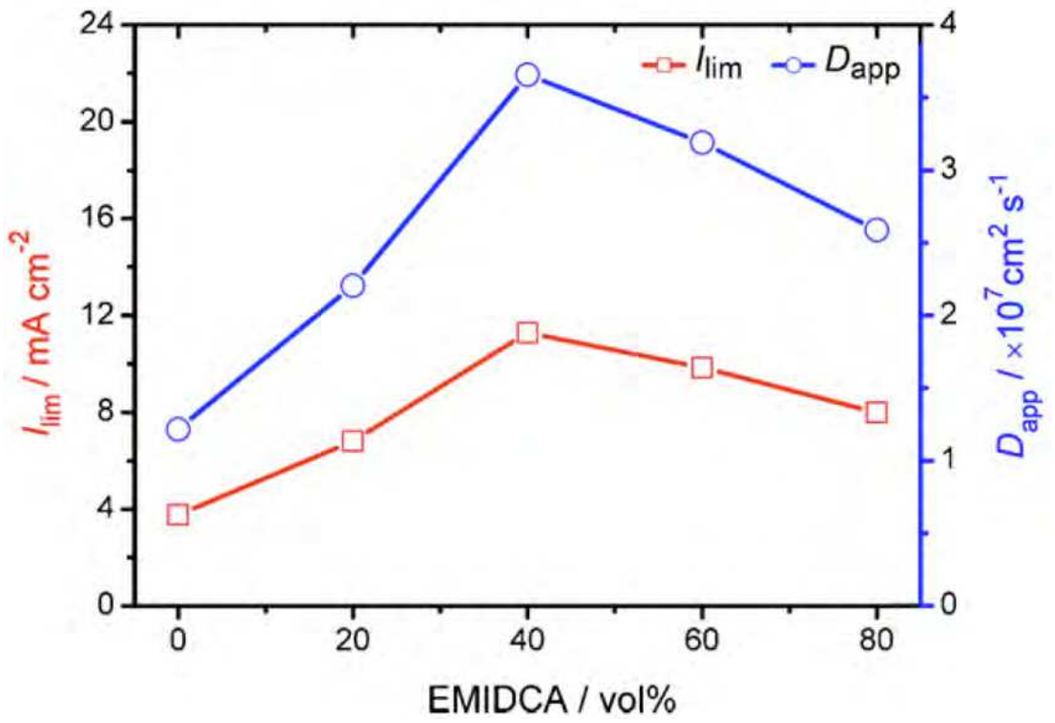

Fig. 13. Dependence of the limiting current density and the apparent diffusion coefficient on the EMIDCA volume fraction in the binary IL electrolyte. Reproduced from (Hao *et al.*, 2011), with permission.

Since 1991, numerous liquid electrolytes have been tested in DSSCs (often by varying the counterion), with the most efficient yielding cells with about 11% efficiency (W. Peng *et al.*, 2003; Hao *et al.*, 2011). However, Grätzel noted that the presence of a liquid solvent for the electrolyte requires "hermetic" sealing of the module in order to prevent evaporation of the volatile solvent (Kay *et al.*, 1996). Such processes are difficult and costly to perform, and mitigate the ease of fabrication that makes DSSCs an attractive alternative to silicon solar cells. The necessity to create a vacuum within the cell and backfill with liquid electrolyte requires slow heating and cooling in order to avoid cracking the glass, and large modules would require significant mechanical strength in order to hold up against bending under wind load. It has also been shown that the I^-/I_3^- redox couple is highly reactive and corrosive with the other components of the DSSCs, especially the sealing material (I. Lee *et al.*, 2010). Finally, the disproportionation reaction of I_2^- has a redox energy that is much higher than the reaction between dye and iodide – this reaction lies closer in energy to the TiO_2 conduction band edge. Thus, the energy difference between HTL and ETL is made smaller by this reaction, and it in fact accounts for an approximately 0.75V loss in maximum photovoltage (Boschloo *et al.*, 2009).

5.2 Ionic liquids as HTL

To address these problems, non-volatile, room-temperature ionic liquid electrolytes have been investigated as hole transporters in DSSCs. These electrolytes have virtually zero vapor pressure in the temperature range experienced inside the cell, although sealing is still required to contain the liquid (Welton *et al.*, 1999). Although these non-volatile liquid electrolytes obviate the need for hermetic sealing, they are by nature very viscous and

incapable of achieving the rapid physical diffusion rates of the solvent-based liquid electrolytes. Using 1-alkyl-3-methylimidazolium iodide as a room-temperature ionic liquid electrolyte (ILE), Yanagida et. al. were able to achieve a device efficiency of 5.0%, as compared to 7.9% when using the redox couple and organic liquids (OGEs). In order to achieve a quasi-solid state device, which is more robust and resistant to leakage over time, they added a gelator to form an ionic gel electrolyte (IGE) (Figure 14), and they observed the same device efficiency of 5.0%. Furthermore, they found that at high temperatures, the IGE cells outperformed the OGEs, due to the thermal stability of the ionic gel electrolyte (Kubo *et al*., 2003). Finally, it was determined that the viscosity of the liquid could be manipulated by varying the alkyl chain length. Longer chains lowered the viscosity of the solution (by interrupting ionic interactions) and led to the most efficient device. Along similar lines, Zakeeruddin et. al. used a mixture of carbon black and PMII-based ionic liquid and obtained a device efficiency of 6.37% (Lei *et al*., 2010). Lianos et. al. cleverly designed a sol-gel process whereby 1-methylimidazole is reacted with 3-iodopropyltrimethoxysilane to form the alkoxysilane derivitized electrolyte and I^-, giving an almost solid state electrolyte (Figure 15). By virtue of its solidity, albeit desirable, this electrolyte resulted in a mediocre device efficiency of only 3.2% (Jovanovski *et al*. 2006).

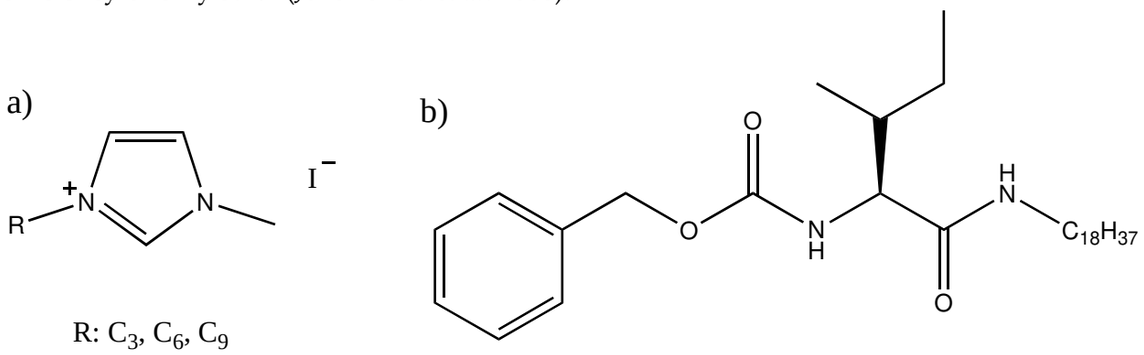

Fig. 14. Chemical Structures of (a) 1-Alkyl-3-methylimidazolium Iodide and (b) Gelator.

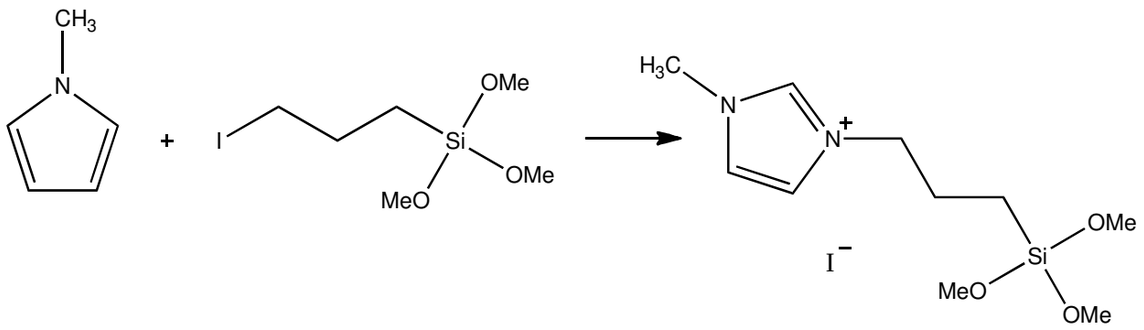

Fig. 15. Synthesis of TMS-PMII by refluxing in 1,1,1-trichloroethane.

5.3 Quasi-solid state HTL

Besides adding gelators to ionic liquids, it is possible to create quasi-solid state electrolytes by incorporating polymers into the electrolyte in a number of creative ways. One such method is to use a polymer to form a host matrix that traps the liquid electrolyte. These devices maintain the high ionic conductivities of liquid electrolytes, but protect against

leakage and physical stress from thermal expansion. This concept was pioneered in 1995 by Searson et. al., who simply polymerized polyacrylonitrile in a mixture containing ethylene carbonate, propylene carbonate, acetonitrile and the desired concentration of NaI. The resulting gel was applied to the counter-electrode of a DSSC and efficiencies of 3-5% were achieved (Cao *et al*., 1995). Since then and continuing today, a variety of polymers and electrolyte combinations have been explored, with reported efficiencies ranging from 2% to 8.2% (Bai *et al*., 2008; Jin *et al*., 2010). This remarkably high efficiency was achieved by Grätzel et. al., who reasoned that a eutectic melt of different polymers would have a lower viscosity than a binary melt or other simple formulations. Yet, despite this result, more recently published papers continue to report much lower efficiencies for polymer-based quasi-solid state devices, suggesting that there is a relatively poor understanding of the factors that lead to a highly effective electrolyte. Continued research in this field looks to be promising, and may eventually lead to devices that surpass the efficiency of liquid electrolyte systems at operating temperatures.

5.4 Solid state HTL

Even in quasi-solid-state devices, sealing is necessary to contain the liquid electrolyte. In order to completely preclude this necessity, it is possible to create solid-state DSSCs (ss-DSSCs) with completely solid-state materials, namely small molecules and conjugated polymers. Small molecules can be inorganic, such as the copper salts CuI and CuSCN, or entirely organic, such as SpiroMeOTAD (2,2′,7,7′-tetrakis(N,N-di-p-methoxyphenyl-amine)9,9′-spirobifluorene) (Bach *et al*., 1998). Solutions of these molecules are given time to permeate the TiO_2, and then the solvent is evaporated, leaving only the solute molecules. However, device efficiencies with these materials are generally poor – devices using SpiroMeOTAD hover around 5% efficiency (Ding *et al*., 2009). Although hole transport in ss-DSSCs is not fully understood, it is postulated that these materials function poorly because they transport charge electronically, as opposed to ionically. Studies suggest that the ionic nature of liquid electrolytes is critical to their high efficiency (Nogueira *et al*., 2001).

Polyelectrolytes are a relatively recent innovation, in principle able to exploit both the efficiency advantages of ionic conduction and the stability of solid-state materials. The polyelectrolytes used are typically non-conjugated polymers containing covalently bound charged groups. Like other solid-state devices, they still suffer from diminished efficiencies because charge transport, while ionic, relies entirely on exchange reactions and not diffusion. Unfortunately, polymers are large and often unable to penetrate the TiO_2 matrix and contact the dye, so they must often be synthesized *in situ* for contact with the dye, and afterwards there is little or no further diffusion into the pore spaces. In 2001, De Paoli *et. al*. introduced the first solid state device using polyelectrolytes, achieving a maximum efficiency of only 2.6% under low-light conditions (Nogueira *et al*., 2001). Since then, despite numerous attempts, the efficiency of such devices has generally remained low. In 2010, Jin et. al. achieved a device efficiency of only 2.42% (Jin *et al*., 2010). These materials, however, still provide much promise for future improvement. Their performance is limited primarily by the decreased diffusion rates of the electrolytes they contain. With the discovery of new, more intensely absorbing dyes, the required thickness of DSSCs will decrease, mitigating the significance of electrolyte viscosity (Kubo *et al*.,

2003). As this happens, quasi-solid state electrolytes may become increasingly competitive with liquid electrolytes.

Conjugated polymers are a widely-used material in solid-state hole transport devices, though like all solid-state devices they remain fairly inefficient compared to liquid electrolyte cells. However, they hold promise for being stable, efficient solid-state hole transport-devices. These materials, which are characterized by a long, delocalized pi-bond system along their carbon backbone, are able to transport holes through their valence band. Many polymers have emerged, most notably polythiophenes such as Poly(3,4-ethylenedioxythiophene) poly(styrenesulfonate) (PEDOT:PSS). Recent work with graphene / PEDOT:PSS - coated cathodes has yielded cells with 4.5% efficiencies (Hong *et al*., 2008). As well, these materials are often able to catalyze hole transport in liquid devices by providing an extra electronic step in between liquid electrolyte redox potential and cathode. In 2009, Cheng et. al. fabricated a counter-electrode from PEDOT:PSS, which catalyzed the regeneration of iodide at the counter-electrode and achieved an efficiency of 5.25% (Sirimanne *et al*., 2010).

Though still a relatively low-efficiency component in DSSCs compared to liquid electrolytes, conjugated polymers provide a wealth of opportunities for improvement and experimentation. Work has been done in the Johal lab at Pomona College on the tuning of photoactive conjugated polyelectrolytes. These materials are adept at transferring holes through their HOMO, but are also excited in the visible range, and have charged side-groups that allow them to be tuned via surfactants. Work by Treger *et al* has shown that adding surfactant lowers the optical band gap of these polymers (presumably by increasing the effective conjugation length), improves internal quantum efficiency, and decreases photooxidation and degradation (Treger *et al*, 2008a, 2008b).

Recent work by Polizzotti, DeJong, Schual-Berke, and Johal has attempted to examine the effects on efficiency of adding the conjugated polyelectrolyte Poly[5-methoxy-2-(3-sulfopropoxy)-1,4-phenylenevinylene] (MPS-PPV) to a liquid electrolyte-based cell. Though a marked increase in current and cell performance is observed (especially upon the addition of surfactant), voltammetric and spectroscopic analyses of these materials show hole transport from iodine redox couple to polymer to be forbidden (see figure 16a). To rectify this discrepancy, a mechanism in which the photoactive polyelectrolyte is generating a second exciton to facilitate hole transport is proposed and shown in figure 16b. As of yet, little to no work has been done on the subject of dual exciton generation in DSSCs. It is hoped, however, that this study will inspire further investigation into this matter, and prove to be yet another way of tuning and optimizing hole transport in DSSCs.

Liquid electrolytes remain the most efficient HTL to date. However, from a mechanical standpoint, solid-state electrolytes are the ideal option for DSSCs due to their improved stability. The main drawback of these materials is that they have yet to prove their viability as effective charge transporters, and a wealth of new research is based on creation of an optimal solid-state DSSC. Conjugated polymers, small-molecule solid HTLs, and others all show promise to provide the next breakthrough in ss-DSSCs, while quasi-solid-state gel electrolyte systems combine the benefits of polymeric materials and liquid electrolytes, also provide promise of high-efficiency, long-lived DSSCs. It is unclear which type of HTL will become the dominant technology, but it will surely have a drastic impact on the efficiency of DSSCs.

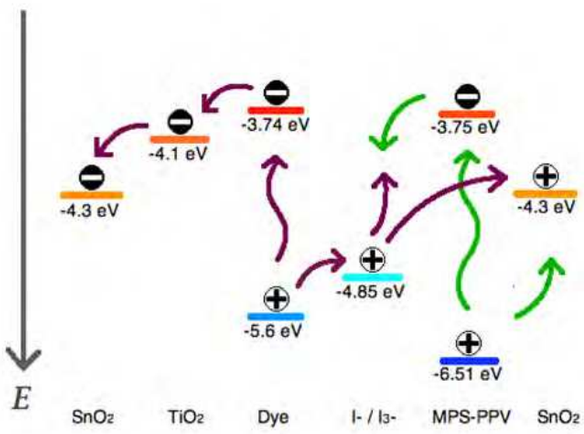

(a)

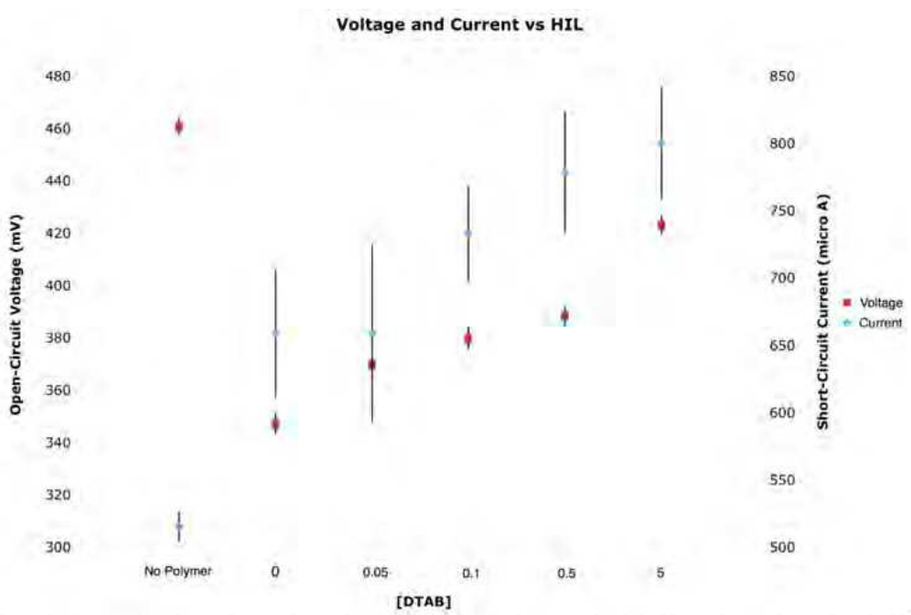

(b)

Fig. 16. Cells fabricated using both liquid iodine and a photoactive polymer HTL. (a) Current and voltage data for cells using MPS-PPV with varying concentrations of the surfactant DTAB. Current increases upon addition of polymer, and a 42+/- 12% increase in max power ($V_{oc}xJ_{sc}$) is observed when films of MPS-PPV with 5 mM DTAB are added to the cell. (b) Proposed electron flow mechanism involving secondary exciton generation by photoactive polymer HTL. Energy values are vs. vacuum and refer to MPS-PPV with [DTAB] = 0.

6. Conclusion

Grätzel cells are poised to become an important player in photovoltaic energy generation. They have already achieved over 11% efficiencies in prototype champion cells. Their watt-

to-cost ratio promises to be very favorable, especially with the recent introduction of ruthenium-free dyes. As advances are made in more effective semiconductor morphologies, lower-cost, higher-efficiency dyes, and more effective and long-lasting hole conduction materials, these devices grow ever closer to commercial viability. However, there is still work to be done before these cells can start producing cheap, clean energy on a larger scale. In this chapter we described the functions and challenges for each of the components of a Grätzel cell, and outlined research needed for new and innovative ways of separating and transporting charges within these devices. By having a full understanding of the drawbacks facing DSSCs and the ways that current research is attempting to address them, can future experimenters be poised to discover the next groundbreaking solutions.

7. Acknowledgments

The authors would like to thank the Pomona College chemistry department for resources to conduct our research as well as their unending support. They would also like to thank the other members of the Johal lab for advice and assistance in and out of the lab.

8. References

Adachi, M., Murata, Y., Okada, I., & Yoshikawa, S.J. (2003). *Electrochem. Soc.* Vol. 150, No. 8, (June 2003), pp. G488-G493. ISSN 0013-4651

Bach, U., Lupo, D., Comte, P., Moser, J., Weissortel, F., Salbeck, J., Spreitzer, H., & Grätzel, M. (1998). Solid-state dye-sensitized mesoporous TiO_2 solar cells with high photon-to-electron conversion efficiencies. *Nature*, Vol. 395, No. 6702, (October 1998), pp. 583-585

Bai, Y., Cao, Y., Zhang, J., Wang, M., Li, R., Wang, P., Zakeeruddin, S., & Grätzel, M. (2008). High-performance dye-sensitized solar cells based on solvent-free electrolytes produced from eutectic melts. *Nat. Mater.* Vol. 7, No. 8, (June 2008), 626-630

Bendall, J.S., Etgar, L., Tan, S.C., Cai, N., Wang, P., Zakeeruddin, S.M., Grätzel, M., & Welland, M.E. (2011). An Efficient DSSC Based on ZnO Nanowire Photo-anodes and a New D-p-A Organic Dye. *Royal Soc. Chem.*, (May 2011)

Bessho, T., Zakeeruddin, S., Yeh, C., Diau, E., & Grätzel, M. (2010). Highly Efficient Mesoscopic Dye-Sensitized Solar Cells Based on Donor – Acceptor-Substituted Porphyrins. *Angewandte Chemie.* Vol.122, (2010) pp. 6796-6799

Cahen, D., Hodes, G., Grätzel, M., Guillemoles, J.F., & Riess, I. (2000). Nature of Photovoltaic Action in Dye-Sensitized Solar Cells. *J Phys Chem B*, Vol. 104, No. 9 (February 2000), pp. 2053-2059.

Calogero, G. & Di Marco, G. (2008). Red Sicilian orange and purple eggplant fruits as natural sensitizers for dye-sensitized solar cells. *Solar Energy Materials & Solar Cells*, Vol.92, No.11, (November 2008), pp. 1341-1346. ISSN 0927-0248

Calogero, G., Di Marco, G., Caramori, S., Cazzanti, S., Argazzi, R., & Bignozzi, C. (2009). Natural dye sensitizers for photoelectrochemical cells. *Energy & Environmental Science*, Vol.2, No.11, (August 2009), pp. 1162-1172

Cao, F., Oskam, G., & Searson, P. A solid state, dye sensitized photoelectrochemical cell. *J. Phys. Chem.* Vol. 99, No. 47, (October 1995), pp. 17071-17073. ISSN 0022-3654

Chen, K., Hong, Y., Chi, Y., Liu, W., Chen, B., & Chou, P. (2009). Strategic design and synthesis of novel tridentate bipyridine pyrazolate coupled Ru(II) complexes to

achieve superior solar conversion efficiency. *Journals of Materials Chemistry*, Vol.19, No.30, (April 2009), pp. 5329-5335

Chiba, Y., Islam, A., Watanabe, Y., Komiya, R., Koide, N., & Han, L. (2006). Dye-sensitized solar cells with conversion efficiency of 11.1. *Japanese Journal of Applied Physics,* Vol.45, No.25, (June 2006), pp. 638-640, ISSN 0021-4922

Chiragwandi, Z.G., Gillespie, K., Zhao, Q.X., & Willander, M. (2006). Ultraviolet driven negative current and rectifier effect in self-assembled green fluorescent protein device. *Applied Physical Letters,* Vol. 89, (October 2006), pp. 162909, ISSN 0003-6951

Artificial Photosynthesis in Solar Cells, In: *Connect-Green*, 02.06.2011, available from: <http://www.connect-green.com/artificial-photosynthesis-in-solar-cells/>

Desilvestro, H. & Hebting, Y. Ruthenium-based dyes for Dye Solar Cells, In: *Sigma-Aldrich: Analytical, Biology, Chemistry & Materials Science Products and Services,* 02.06.2011, Available from: <http://www.sigmaaldrich.com/materials-science/organic-electronics/dye-solar-cells.html>

Dierks, S. (May 2006). Ruthenium Material Safety Data Sheet, In: E*SPI Metals*, 03.06.2011, Available from: http://www.espimetals.com/index.php/online-catalog/237-ruthenium

Ding, I.K., Tétreault, N., Brillet, J., Hardin, B., Smith, E., Rosenthal, S., Sauvage, F., Grätzel, M., & McGehee, M. (2009). Pore-filling of spiro-OMeTAD in solid-state dye sensitized solar cells: quantification, mechanism, and consequences for device performance. *Adv. Funct. Mater.* Vol. 19, No. 15, (2009), pp. 1-6

Duffy, N. W., Peter, L.M., Rajapakse, R.M.G., & Wijayantha, K.G.U. (2000). A Novel Charge Extraction Method for the Study of Electron Transport and Interfacial Transfer in Dye Sensitized Nanocrystalline Solar Cells. *Electrochemistry Communications* Vol. 2, (June 2000), pp. 658-662. ISSN 1388-2481

de Freitas, J.N., Nogueira, A., & De Paoli. M. (2009). New insights into dye-sensitized solar cells with polymer electrolytes. *J. Mater. Chem.*, Vol. 19, No. 30, (May 2009), pp. 5279-5294

Ghadiri, E., Taghavinia, N., Zakeeruddin, S.M., Grätzel, M., & Moser, J.E. (2010) Enhanced Electron Collection Efficiency in Dye-Sensitized Solar Cells Based on Nanostructured TiO2 Hollow Fibers. *Nano Letters*, Vol. 10, (April 2010), pp. 1632-638.

Grätzel, M. (2004). Conversion of sunlight to electric power by nanocrystalline dye-sensitized solar cells. *Journal of Photochemistry and Photobiology A,* Vol.164, No.1-3, (June 2004), pp. 3-14. ISSN 1010-6030

Grätzel, M. (2005). Solar Energy Conversion by Dye-Sensitized Photovoltaic Cells. *Inorganic Chemistry,* Vol.44, No.20, (October 2005), pp. 6841-6851

Green, M.A. (1981) Solar cell fill factors: General graph and empirical expressions. *Solid-State Electronics*, Vol. 24, No. 8, (August 1981), pp. 788 – 789. ISSN 0038-1101

Hao, F., Lin, H., Zhang, J., & Li, J. (2011). Balance between the physical diffusion and the exchange reaction on binary ionic liquid electrolyte for dye-sensitized solar cells. *J. Power Sources.* Vol. 196, No. 3, (February 2011), pp. 1645-1650. ISSN 0378 7753

Helgesen, M., Søndergaard, R., & Krebs, F. (2009). Advanced materials and processes for polymer solar cell devices. *J. Mater. Chem.* Vol. 20, No. 1, (October 2009), pp. 36-60

Hong, W., Xu, Y., Lu, G., Li, C., & Shi, G. (2008). Transparent graphene / PEDOT-PSS composite films as counter electrodes of dye-sensitized solar cells, *Electrochem. Communications*, Vol. 10, No. 10, (October 2008), pp. 1555-1558. ISSN 1388-2481

Ito, S., Zakeeruddin, S., Humphry-Baker, R., Liska, P., Charvet, R., Comte, P., Nazeeruddin, M., Péchy, P., Takata, M., Miura, H., Uchida, S., & Grätzel, M. (2006). High-efficiency organic dye-sensitized solar cells controlled by nanocrystalline-TiO_2 electrode thickness. *Advanced Materials,* Vol.18, No.9, (May 2006), pp. 1202-1205

Ito, S., Chen, P., Comte, P., Nazeeruddin, M.K., Liska, P., Péchy P., & Grätzel, M. (2007). Fabrication of screen-printing pastes from TiO_2 powders for dye-sensitized solar cells. *Prog. Photovoltaics* Vol. 15, No. 7, (March 2007), pp. 603–612.

Ito, S., Miura, H., Uchida, S., Takata, M., Sumioka, K., Liska, P., Comte, P., Pechy, P., & Grätzel, M. (2008). High-conversion-efficiency organic dye-sensitized solar cells with a novel inoline dye. *Chemistry Communications*, (September 2008), pp. 5194-5196

Jennings, J.R., Ghicov, A., Peter, L.M., Schmuki, P., & Walker, A.B. (2008). Dye-Sensitized Solar Cells based on Oriented TiO_2 Nanotube Arrays: Transport, Trapping, and Transfer of Electrons. *J. Am. Chem. Soc.*, Vol. 130, (2008), p. 13364.

Jin, X, Tao, J, & Yang, Y. (2010). Synthesis and characterization of poly(1-vinyl-3-propylimidazolium) iodide for quasi-solid polymer electrolyte in dye-sensitized solar cells. *J. Appl. Polym. Sci.* Vol. 118, No. 3, (June 2010), pp. 1455-1461

Johansson, E.M.J., Sandell, A.; Siegbahn, H., Rensmo, H., Mahrov, B., Boschloo, G., Figgemeier, E., Hagfeldt, A., Jonsson, S.K.M., & Fahlman, M. (2005). Interfacial Properties of Photovoltaic TiO2 / Dye / PEDOT-PSS Heterojunctions. *Synthetic Metals*, Vol. 149, (January 2005), pp. 157-167. ISSN 0379-6779

Jovanovski, V., Stathatos, E., Orel, B., & Lianos, P. (2006). Dye-sensitized solar cells with electrolyte based on a trimethoxysilane-derivatized ionic liquid. *Thin Solid Films*, Vol. 511-512, (January 2006), pp. 634-637. ISSN 0040-6090

Katoh, R., Yaguchi, K., Murai, M., Watanabe, S., & Furube, A. (2010). Differences in adsorption behavior of N3 dye on flat and nanoporous TiO_2 surfaces, *Chem. Phys. Letters*, Vol. 497, No. 1-3, (July 2010), pp. 48-51. ISSN 0009-2614

Kay, A., & Grätzel, M. (1996). Low cost photovoltaic modules based on dye sensitized nanocrystalline titanium dioxide and carbon powder. *Sol. Energ. Mat. Sol. C.* Vol. 44, No. 1, (October 1996), pp. 99-117. ISSN 0927-0248

Kuang, D., Uchida, S., Humphry-Baker, R., Zakeeruddin, S.M., & Grätzel, M. (2008). Organic Dye-Sensitized Ionic Liquid Based Solar Cells: Remarkable Enhancement in Performance through Molecular Design of Indoline Sensitizers, *Angewandte Chemie International Edition*, Vol. 47, No. 10, (February 2008), pp. 1923-1927

Kubo, W., Kambe, S., Nakade, S., Kitamura, T., Hanabusa, K., Wada, Y., & Yanagida, S. (2003). Photocurrent-determining processes in quasi-solid-state dye-sensitized solar cells using ionic gel electrolytes. *J. Phys. Chem. B.* Vol. 107, No. 18, (April 2003), pp. 4374-4381

Lee, G.W., Kim, D., Ko, M.J., Kim, K., & Park, N.G. (2010). Evaluation on over photocurrents measured from unmasked dye-sensitized solar cells, *Solar Energy*, Vol. 84, (January 2010), pp. 418-425. ISSN 0038-092X

Lee, I., Hwang, S., & Kim, H. (2010). Reaction between oxide sealant and liquid electrolyte in dye-sensitized solar cells. *Sol. Energ. Sol. Mat. C.* Vol. 95, No. 1, (2011), pp. 315-317. ISSN 0927-0248

Lei, B.X.., Fang, W., Hou, Y., Liao, J., Kuang, D., & Su, C. (2010). All-solid-state electrolytes consisting of ionic liquid and carbon black for efficient dye-sensitized solar cells. *J. Photoch. Photobio. A.* Vol. 216, No. 1, (September 2010), pp. 8-14. ISSN 1010-6030

Ruthenium (Ru) – Chemical properties, health and environmental effects, In: *Water Treatment Solutions - Lenntech*, 03.06.2011, Available from: http://www.lenntech.com/periodic/elements/ru.htm

Li, B., Wang, L., Kang, B., Wang, P., & Qiu, Y. (2006). Review of recent progress in solid-state dye-sensitized solar cells. *Sol. Energ. Mat. Sol. C.* Vol. 90, No. 5, (2006), pp. 549-573. ISSN 0927-0248

Li, S., Liu, Y., Zhang, G., Zhao, X., & Yin, J. (2011). The role of the TiO2 nanotube array morphologies in the dye-sensitized solar cells, *Thin Solid Films* (2011). ISSN 0040-6090

Liu, G., Jaegermann, W., He, J., Sundstrom, V., & Sun, L. (2002). XPS and UPS Characterization of the TiO2/ZnPcGly Heterointerface: Alignment of Energy Levels. *J. Phys. Chem. B* Vol. 106, (May 2002), pp. 5814-5819.

Mor, G.K., Shankar, K., Paulose, M., Varghese, O.K., & Grimes, C.A. (2006). Use of Highly-Ordered TiONanotube Arrays in Dye-Sensitized Solar Cells. *Nano Letters*, Vol. 6, No. 2, (2006), pp. 215-218.

Nazeeruddin, M.K., Kay, A., Rodicio, I., Humphry-Baker, R., Muller, E., Liska, P., Vlachopouslos, N., & Grätzel, M. (1993). Conversion of Light to Eelectricity by *cis*-X_2Bis(2,2′-bipyridyl-4,4′-dicarboxylate)ruthenium(II) Charge-Transfer Sensitizers (X = Cl^-, Br^-, I^-, CN^-, and SCN^-) on Nanocrystalline TiO_2 Electrodes. *J. Am. Chem. Soc.* Vol. 115, (July 1993), pp. 6382-6390. ISSN 0002-7863

Neild, B. (2010). Jellyfish' Smoothies Offer Solar Solutions. In: *CNN.com*, May 2011, Available from: <http://www.cnn.com/2010/TECH/innovation/09/27/jellyfish.solar.power/index.html>

Nogueira, A., Durrant, J., & De Paoli, M. (2001). Dye-sensitized nanocrystalline solar cells employing a polymer electrolyte. *Adv. Mater.* Vol. 13, No. 11, (June 2001), pp. 826 – 830. ISSN 0935-9648

O'Regan, B., & Grätzel, M. (1991). A Low-cost, High-efficiency Solar Cell Based on Dye-sensitized Colloidal TiO2 Films. *Nature* Vol. 353, No. 6346, (October 1991), pp. 737-740

Peng, B., Jungmann, G., Jager, C., Haarer, D., Schmidt, H.W., & Thelakkat, M. (2004). Systematic Investigation of the Role of Compact TiO2 Layer in Solid State Dye-sensitized TiO2 Solar Cells. *Coordination Chemistry Reviews*, Vol. 248, No. 13-14, (June 2004), pp. 479-489. ISSN 0010-8545

PVEducation. (2010). Fill Factor. In: *Pveducation.org*. Web. 07 June 2011. Available from: <http://www.pveducation.org/pvcdrom/solar-cell-operation/fill-factor>

Ryan, M. (2009). Progress in ruthenium complexes for dye sensitised solar cells. *Platinum Metals Review*, Vol.53, No.4, (October 2009), pp. 216-218

Saito, Y. (2004). Solid State Dye Sensitized Solar Cells Using in Situ Polymerized PEDOTs as Hole Conductor. *Electrochemistry Communications* Vol. 6, No. 1, (2004), pp. 71-74. ISSN 1388-2481

Schoonman, J. (2005). Nano-structured materials for the conversion of sustainable energy, In: *Nanostructured and advanced materials for applications in sensor, optoelectronic and photovoltaic technology,* Vaseashta, A., Dimova-Malinovska, D., & Marshall, J., pp. 270-280

Singh, P.K., Kim, K.W., Park, N.G., & Rhee, H.W. (2008). Mesoporous nanocrystalline TiO_2 electrode with ionic liquid-based solid polymer electrolyte for dye-sensitized solar cell application, *Synthetic Materials*, Vol. 158, No. 14, (August 2008), pp. 590-593. ISSN 0379-6779

Sirimanne, P.M., Winther-Jensen, B., Weerasinghe, H.C., & Cheng, Y.B. (2010). Towards an all-polymer cathode for dye sensitized photovoltaic cells, *Thin Solid Films*, Vol. 518, No. 10, (March 2010), pp. 2871-2875. ISSN 0040-6090

Smestad, G.P. (2003). A Technique to Compare Polythiophene Solid-State Dye Sensitized TiO_2 Solar Cells to Liquid Junction Devices. *Solar Energy Materials and Solar Cells*, Vol. 76, (April 2003), pp. 85-105. ISSN 0927-0248

Ruthenium Dyes, In: *Solaronix Products*, 03.06.2011, Available from: <http://www.solaronix.com/products/dyes/>

Tang, H., Berger, H., Schmid, P.E., & Levy, F. (1994). Optical Properties of Anatase (TiO2). *Solid State Communications*, Vol. 92, No. 3, (June 1994), pp. 267-271. ISSN 0038-1098

Treger, J.S., Ma, V.Y., Gao, Y., Wang, C.C., Wang, H.L., & Johal, M.S. (2008a). Tuning the optical properties of a water-soluble cationic poly(*p*-phenylenvinylene): surfactant complexation with a conjugated polyelectrolyte, *J.Phys. Chem. B.*, Vol. 112, (January 2008), pp. 760-763.

Treger, J.S., Ma, V.Y., Gao, Y., Wang, C.C., Jeon, S., Robinson, J.M., Wang, H.L., & Johal, M.S. (2008b). Controlling layer thickness and photostability of water-soluble cationic poly(*p*-phenylenevinylene) in miltilayer thin films by surfactant complexation, *Langmuir*, Vol. 24, (August 2008), pp. 13127-13131

Wang, P., Zakeeruddin, S., Moser, J., Nazeeruddin, M., Sekiguchi, T., & Grätzel, M. (2003). A stable quasi-solid-state dye-sensitized solar cell with an amphiphilic ruthenium sensitizer and polymer gel electrolyte. *Nat. Mater.* Vol. 2, No. 7, (June 2003), pp. 402-407

Wang, P., Zakeeruddin, S, Moser, J, & Grätzel, M. (2003). A new ionic liquid electrolyte enhances the conversion efficiency of dye-sensitized solar cells. *J. Phys. Chem. B.* Vol. 107, No. 48, (September 2003), pp. 13280-13285

Wang, X., Koyama, Y., Kitao, O., Wada, Y., Sasaki, S., Tamiaki, H., & Zhou, H. (2010a). Significant enhancement in the power-conversion efficiency of chlorophyll co-sensitized solar cells by mimicking the principles of natural photosynthetic light-harvesting complexes. *Biosensors and Bioelectrics*, Vol.25, No.8, (April 2010), pp. 1970-1976.

Wang, X., Tamiaki, H., Wang, L., Tamai, N., Kitao, O., Zhou, H., & Sasaki, S. (2010b). Chlorophyll-*a* derivatives with various hydrocarbon ester groups for efficient dye-sensitized solar cells: static and ultrafast evaluations on electron injection and charge collection processes. *Langmuir*, Vol.26, No.9, (May 2010), pp. 6320-6327

Welton, T. (1999). Room-temperature ionic liquids. Solvents for synthesis and catalysis. *Chem. Rev.* Vol. 99, No. 8, (April 1999), pp. 2071-2083

Yanagida, S., & Yu, Y. (2009). Manseki, K. Iodine/iodide-free dye-sensitized solar cells. *Accounts Chem. Res.* Vol. 42, No. 11, (November 2009), pp. 1827-1838

Yum, J., Jang, S., Walter, P., Geiger, T., Nüesch, F., Kim S., Ko, J., Grätzel, M., & Nazeeruddin, M. (2007). Efficient co-sensitization of nanocrystalline TiO_2 films by organic sensitizers, *Chemical Communications*, Vol.44, (November 2007), pp. 4680-4682

Yum, J., Hagberg, D., Moon, S., Karlsson, K., Marinado, T., Sun, L., Hagfeldt, A., Nazeeruddin, M., & Grätzel, M. (2009). A light-resistant organic sensitizer for solar-cell applications, *Angewandte Chemie International Edition*, Vol.48, No.9, (February 2009), pp. 1576-1580

Zafer, C., Karapire, C., Sariciftci, S.N., & Icli, S. (2005). Characterization of N, N0-bis-2-(1-hydoxy-4- Methylpentyl)-3, 4, 9, 10-perylene Bis (dicarboximide) Sensitized Nanocrystalline TiO2 Solar Cells with Polythiophene Hole Conductors. *Solar Energy Materials & Solar Cells* Vol. 88, (October 2005), pp. 11-21. ISSN 0927-0248

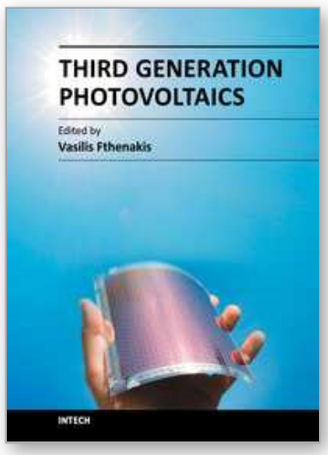

Third Generation Photovoltaics

Edited by Dr. Vasilis Fthenakis

ISBN 978-953-51-0304-2
Hard cover, 232 pages
Publisher InTech
Published online 16, March, 2012
Published in print edition March, 2012

Photovoltaics have started replacing fossil fuels as major energy generation roadmaps, targeting higher efficiencies and/or lower costs are aggressively pursued to bring PV to cost parity with grid electricity. Third generation PV technologies may overcome the fundamental limitations of photon to electron conversion in single-junction devices and, thus, improve both their efficiency and cost. This book presents notable advances in these technologies, namely organic cells and nanostructures, dye-sensitized cells and multijunction III/V cells. The following topics are addressed: Solar spectrum conversion for photovoltaics using nanoparticles; multiscale modeling of heterojunctions in organic PV; technologies and manufacturing of OPV; life cycle assessment of OPV; new materials and architectures for dye-sensitized solar cells; advances of concentrating PV; modeling doped III/V alloys; polymeric films for lowering the cost of PV, and field performance factors. A panel of acclaimed PV professionals contributed these topics, compiling the state of knowledge for advancing this new generation of PV.

How to reference

In order to correctly reference this scholarly work, feel free to copy and paste the following:

Alex Polizzotti, Jacob Schual-Berke, Erika Falsgraf and Malkiat Johal (2012). Investigating New Materials and Architectures for Grätzel Cells, Third Generation Photovoltaics, Dr. Vasilis Fthenakis (Ed.), ISBN: 978-953-51-0304-2, InTech, Available from: http://www.intechopen.com/books/third-generation-photovoltaics/investigating-new-materials-and-architectures-for-gr-tzel-cells

INTECH
open science | open minds

InTech Europe
University Campus STeP Ri
Slavka Krautzeka 83/A
51000 Rijeka, Croatia
Phone: +385 (51) 770 447
Fax: +385 (51) 686 166
www.intechopen.com

InTech China
Unit 405, Office Block, Hotel Equatorial Shanghai
No.65, Yan An Road (West), Shanghai, 200040, China
中国上海市延安西路65号上海国际贵都大饭店办公楼405单元
Phone: +86-21-62489820
Fax: +86-21-62489821

IntechOpen